2025 DRAGON 6 SYMPOSIUM

14-18 JULY 2025

[PROJECT ID. 95469]

[TOWARDS FOREST QUALITY ASSESSMENT USING REMOTE SENSING]







ID. 95469

PROJECT TITLE: TOWARDS FOREST QUALITY ASSESSMENT USING REMOTE SENSING

PRINCIPAL INVESTIGATORS: ZUYUAN WANG, TAO YU

CO-AUTHORS: CHRISTIAN GINZLER, LARS. T. WASER, MARIUS RÜETSCHI, ZENGYUAN LI, SHILI MENG , LIMING DU , DAN KONG

PRESENTED BY: ZUYUAN WANG, TAO YU

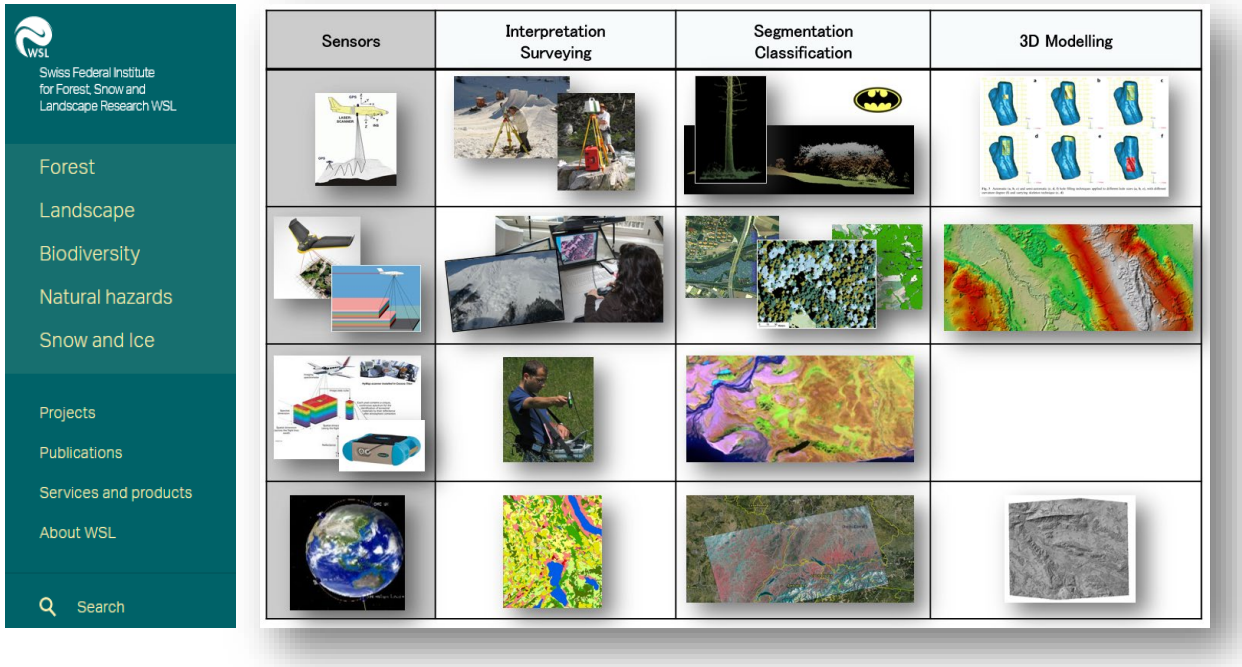
2025 Dragon 6 Symposium

China Part



Institute of Forest Resource Information Techniques,
Chinese Academy of Forestry （IFRIT， CAF）

European Part



Swiss Federal Institute for Forest, Snow and Landscape Research WSL （ Swiss WSL）

2025 Dragon 6 Symposium

1. Background and Objectives
2. Satellite Data
3. In-situ data Measurements and Requirements
4. Schedule, Planning and Contribution of the Partners
5. Training of Young Scientists
6. Overview of YSs research

1. Background and Objectives

- When forests are in good health, they are carbon sinks. Forests may become carbon sources when their adaptability is reduced due to external disturbances.
- Forest quality determines the stability and sustainability of forest ecosystem, and then affects the function of forest ecosystem.





1. Background and Objectives

Questions

- How to estimate forest biomass and forest growth though multi-source remote sensing data?
- How to obtain high-resolution and high-precision forest types through multi-source remote sensing data?

1. Background and Objectives

Objectives

- Generate high-accuracy and high-resolution forest-type classification map
- Monitor forest growth based on multiple datasets
- Estimate vertical forest structure parameters

2. Satellite Data

ESA Third Party Missions	No. Scenes
1. Sentinel-1	20
2. Sentinel-2A/B	20
Total	40

Chinese EO data	No. Scenes
5. TECIS Multi-Angle optimal images	19
6. TECIS Waveform LiDAR data	19
Total	38

2. Satellite Data (China Part)

- Airborne laser scanning (ALS) data from IFRIT



CAF-LiCHy Airborne Observation System (LiDAR-CCD-Hyperspectral)

LiDAR scanner: Riegl VQ580-II			
Wavelength	1064 nm	Laser beam divergence	0.25 mrad
Laser pulse length	3 ns	Scan angle range	±35°
Maximum laser	2000 kHz	Maximun scanning speed Point density@1000 m	300 lines/s 30 pts/m^2
Echo intensity	15 / beam-forming	Vertical accuracy	0.02 m

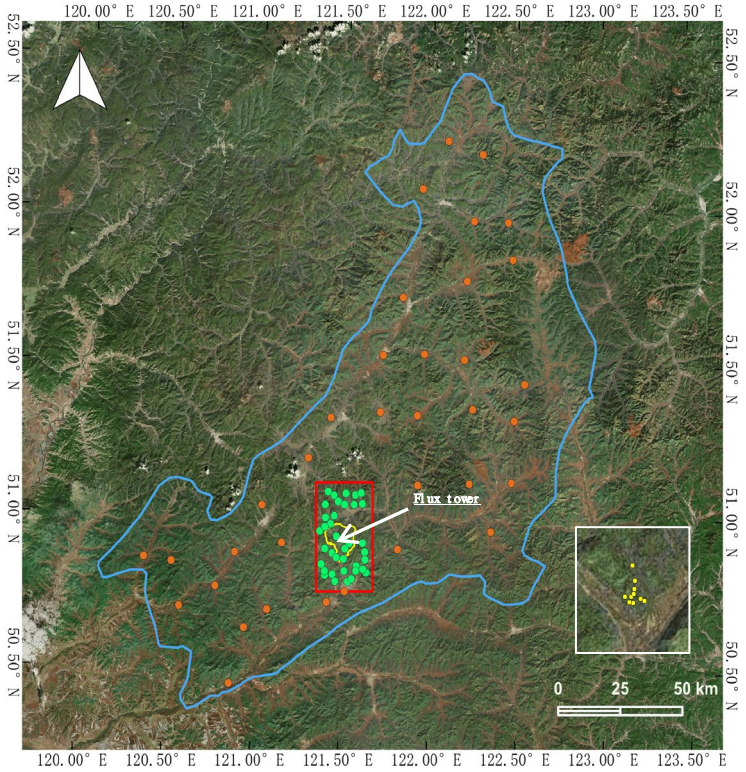
Medium wave infrared (MWIR) camera : InfraTec ImageIR		Long wave thermal infrared (LWIR)camera: InfraTec VarioCam HD	
Wavelength	2.0-5.7μm	Wavelength	7.5-14μm
Spatial pixels	640 x 512	Spatial pixels	1024 x 768
Frame rate	106 Hz	Frame rate	30 Hz
Focal length	28.6mm	Focal length	11.1mm
FOV	33.8°	FOV	46.6°
Temperature resolution	0.02 k	Temperature resolution	0.02 k
Temperature range	-40-1500℃	Temperature range	-40-2000℃

Hyperspectral sensor: Specim Aisa FENIX1K			
Wavelength	380-2500 nm	Spatial pixels	1024
Focal length	18.1mm	Spectral resolution	4.5/12 nm
FOV	40°	Maximum bands	87-348/256
Frame rate	100 lines/s	Output	12/16 bits

3. In-situ data Measurements and Requirements

- Field data collection campaigns and periods in China





Forest types	coniferous forest	broad-leaved forest	mixed forest
Number of plots	29	2	16
Number of trees within plot	45~198	87~104	44~163
Average DBH (cm)	9.34~22.75	11.15~13.4	7.52~19.3
Average tree height (m)	9.86~18.04	11.62~15.12	8.95~16.75
Dominant species	larch	white birch	/
AGBD (t/ha)	34.39~210.22	110.95~112.87	36.80~118.25

3. In-situ data Measurements and Requirements

- Field data collection campaigns ---- Swiss National Forest Inventory
  - **Combined inventory (2-phase)**

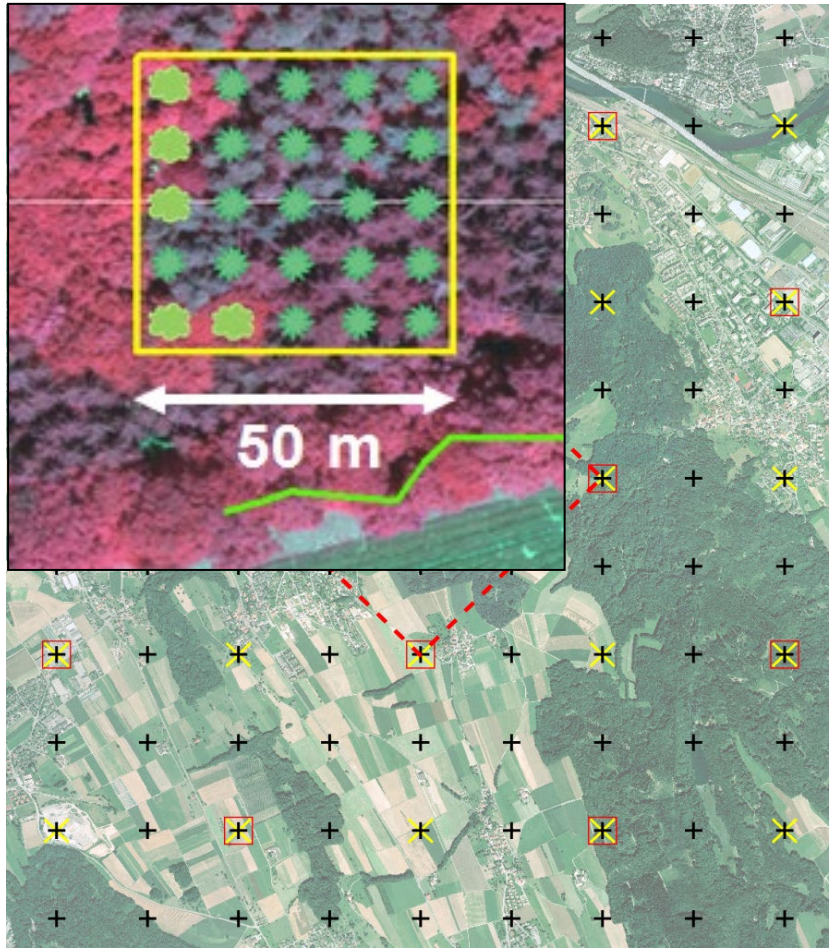
    - Stereo-interpretation of aerial imagery
    - Field surveys (about 6500 field plots / 700 per year)

  - **5 data surveys**

    NFI1: 1983 – 1985 NFI2: 1993 - 1995
    NFI3: 2004 – 2007 NFI4: 2009 – 2018

    NFI5: 2018 – 2026…….





4. Schedule, Planning and Contribution of the Partners

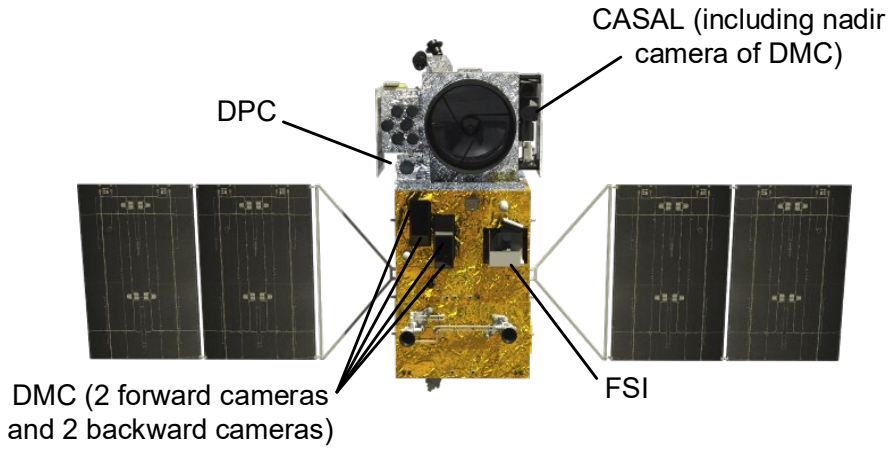
Time	Main work
2024.07~2025.06	• Data collection • Field work • Forest type classification • Forest growth monitoring
2025.07~2026.06	• Airborne flight experiment • Forest gap detection
2026.07~2027.06	• Forest edge effects quantification
2027.07~2028.06	• Forest vertical complexity assessment • Forest quality assessment

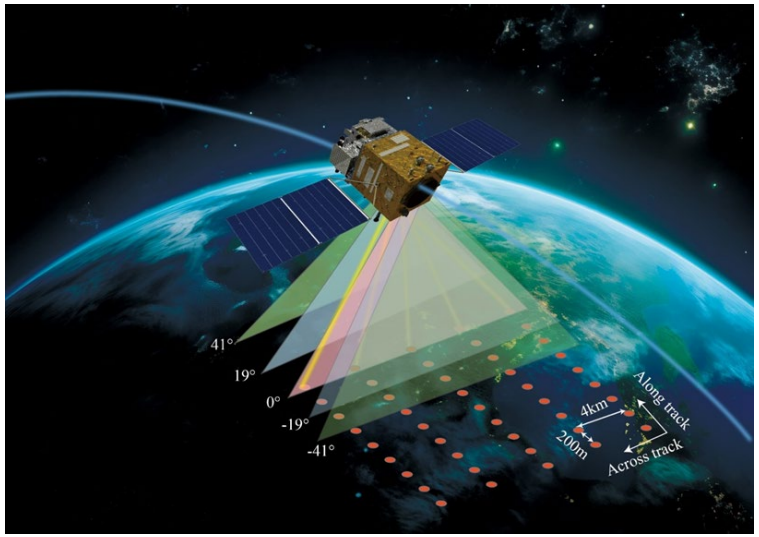
5. Training of Young Scientists

Name	Institution	Poster title	Contribution including period of research
Liming Du	IFRIT/CAF	Monitoring growth of regenerated saplings through stratifying forest overstory using airborne LiDAR data	Forest vertical structure and biomass estimation
Dan Kong	IFRIT/CAF	Aerial LiDAR is all you need for regional forest biomass mapping: progressively synergizing individual-tree and area-based approaches	Forest vertical structure and biomass estimation
Marius Rüetschi	WSL	Forest type classification based on combined Sentinel -1/-2 data	Forest type classification

6. Overview of Chinese YSs research

1. The potential of forest carbon estimation based on TECIS' directional multi-spectral camera data





- Chinese Terrestrial Ecosystem Carbon Inventory Satellite (TECIS) was Launched on August 4th, 2022.
- TECIS is the first mission integrated active and passive sensors for forest carbon mapping.
- TECIS is equipped with a 5-beam LiDAR and a multi-spectral optical camera with 5 viewing angles. It also integrates an optical axis monitoring camera and a hyper-spectral imager for vegetation detection.

6. Overview of Chinese YSs research

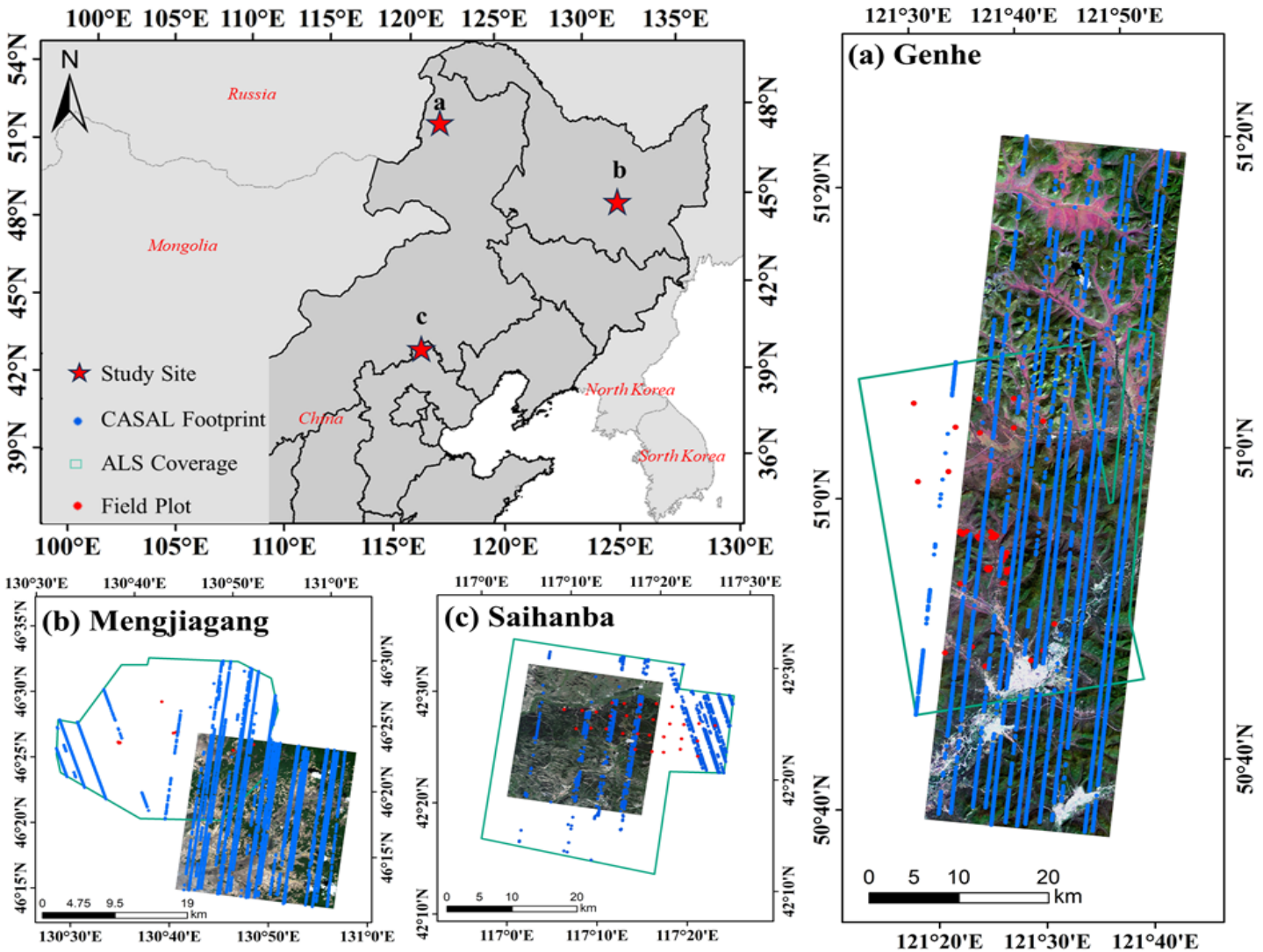
Main parameters of the TECIS Directional Multi-Spectral Camera (DMC)

Camera Name	Pointing angle	Band name	Wavelength	Spatial resolution
F2M	+41°	band 1-4	Same as NAD	12 m
		red-edge band	690~730 nm	6 m
F1M	+19°	band 1-4	Same as NAD	8 m
		PAN	500~760 nm	4 m
NAD	0°	band 1	450~520 nm	2 m
		band 2	520~590 nm	
		band 3	630~690 nm	
		band 4	770~890 nm	
B1M	-19°	band 1-4	Same as NAD	8 m
		PAN	500~760 nm	4 m
B2M	-41°	band 1-4	Same as NAD	12 m
		red-edge band	690~730 nm	6 m

Main parameters of the TECIS CASAL system

Parameter (unit)	CASAL value	GEDI value
Wavelength (nm)	1064	1064
Number of beams	5	8
Number of lasers	5	3
Laser energy (mJ)	70	10
Divergence angle (urad)	50	56
Repetition frequency (Hz)	40	242
Laser pulse width (ns)	5	14
Footprint size (m)	25	25
Vertical resolution (m)	0.125	0.15
Vertical range accuracy (m)	0.3	0.1
Digitization frequency (GHz)	1.2	1
Quantization bits (bit)	12	12
Dynamic range (dB)	40	-
Cross track beam interval	~4 km	600 m
Along track beam interval	200 m	60 m

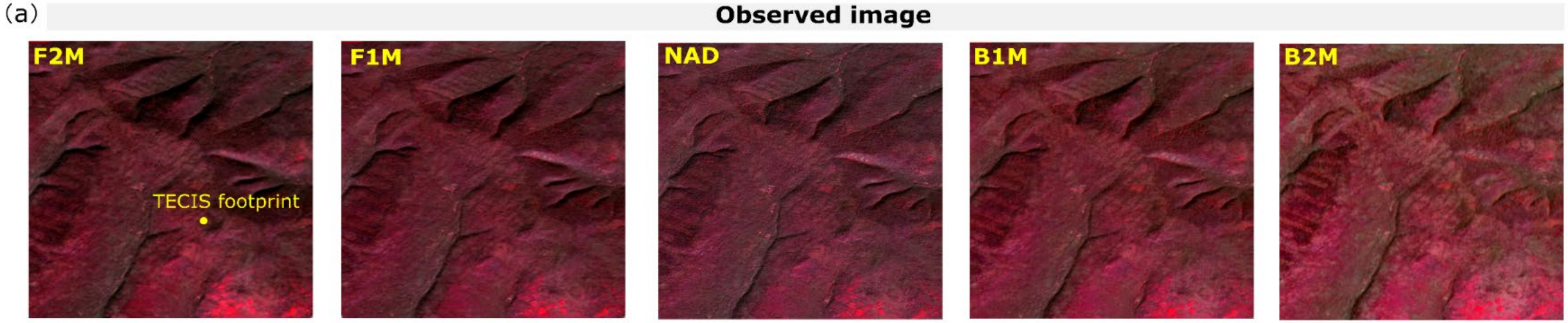
6. Overview of Chinese YSs research



Location of the three study sites in northeast China (top left) with zoom-in views of those sites (a) Genhe, (b) Mengjiagang, (c) Saihanba) showing DMC images and footprints of CASAL LiDAR data (blue dots) acquired by TECIS, coverage of airborne LiDAR data (green polygons), and location of field plot data (red dots).

6. Overview of Chinese YSs research

Raw data -> Radiometric calibration -> RPC geometric correction -> FLAASH atmospheric correction -> BRDF modeling -> Dark and hot spot image reconstruction



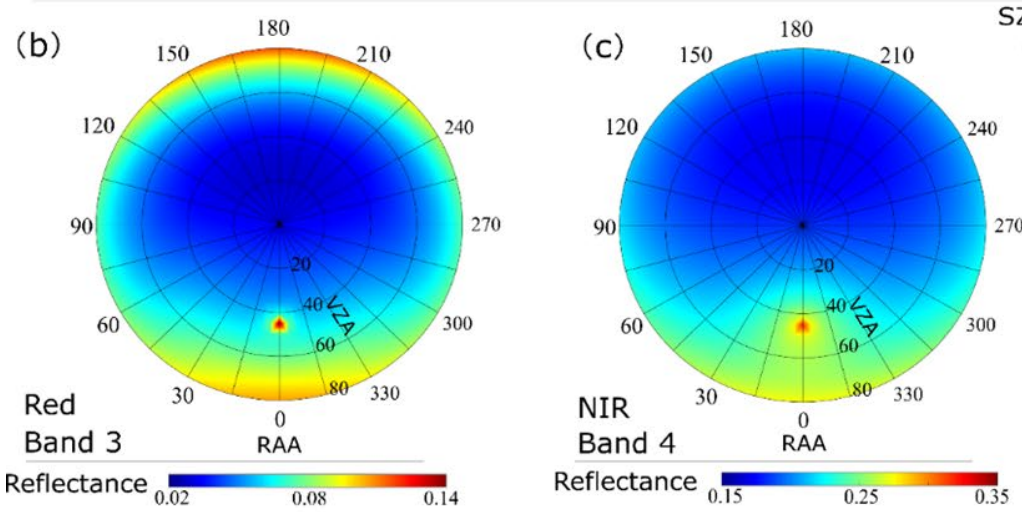
6. Overview of Chinese YSs research

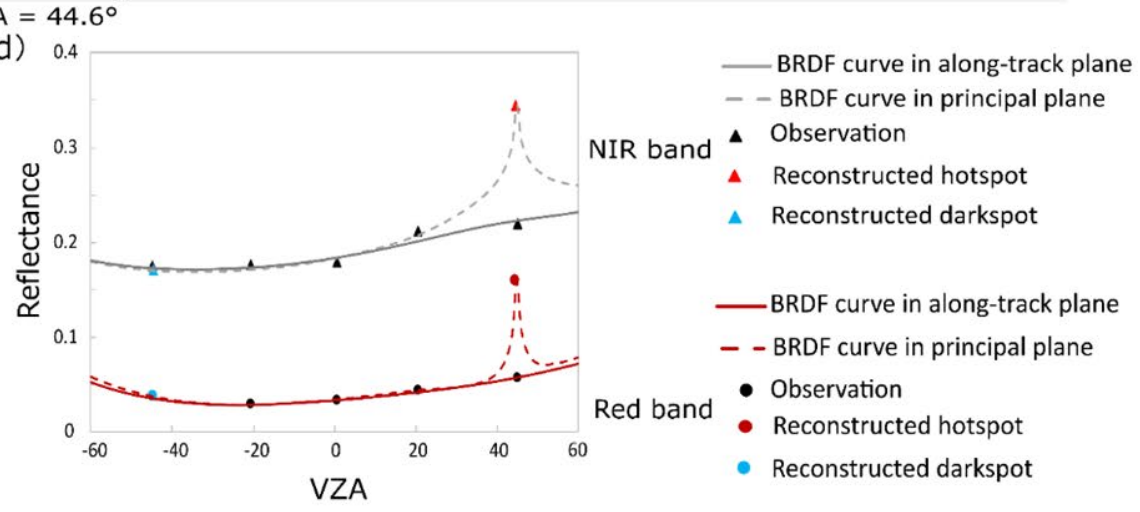


中国科学技术交流中心
China Science and Technology Exchange Center

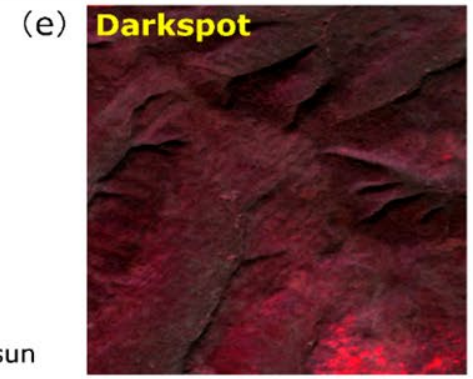
→ THE EUROPEAN SPACE AGENCY

BRDF shape





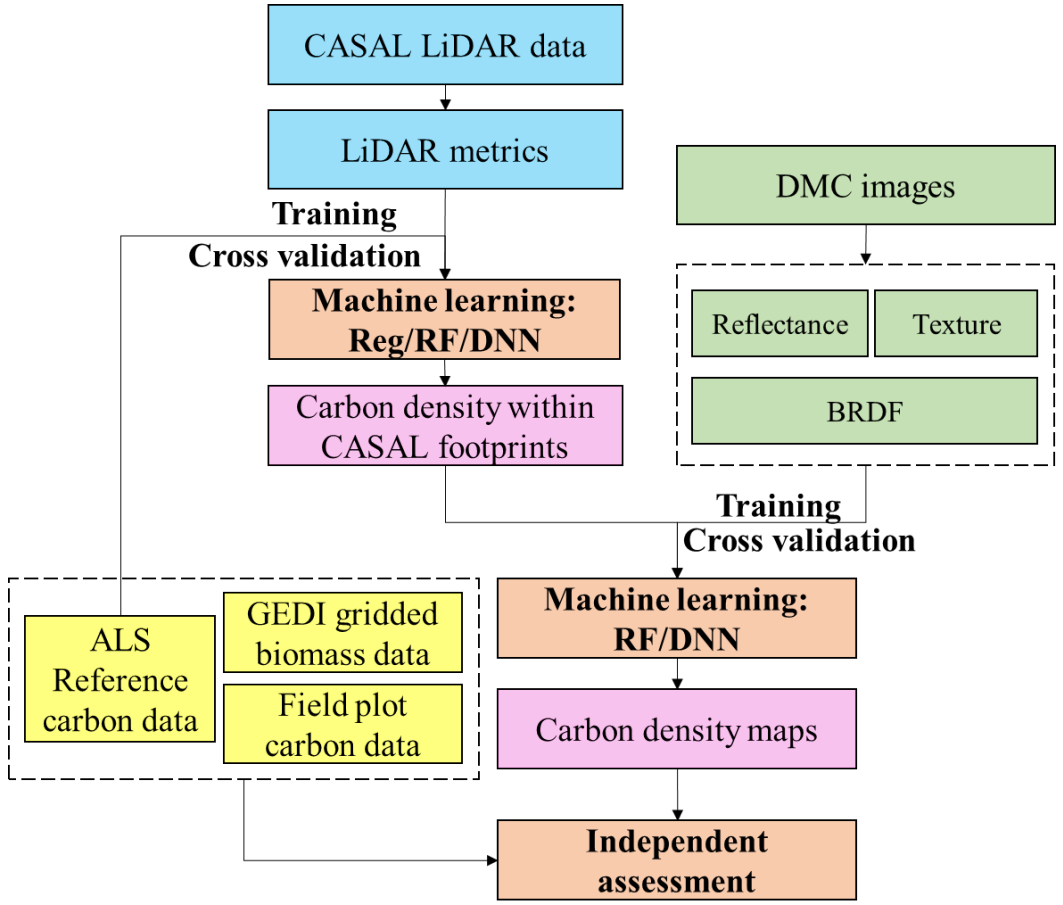
Reconstructed image





VZA: view zenith angle
VAA: view azimuth angle
SZA: solar zenith angle
SAA: solar azimuth angle
RAA : relative azimuth angle between sensor and sun

6. Overview of Chinese YSs research



Flowchart of TECIS forest carbon mapping strategy

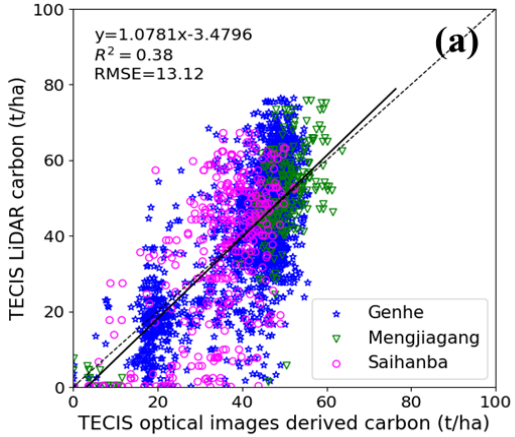
Variables in carbon mapping through CASAL-DMC integration

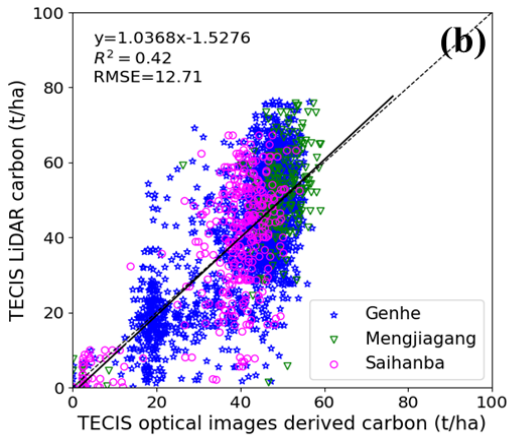
Variable category	Variables	Description	Number of variables
Nadir view (NV) variables	Reflectance	Surface reflectance of nadir view DMC data (4 bands)	4
	Texture-12m Texture-2m	- Fourier-based textural ordination (FOTO): FOTO1, FOTO2, and FOTO3 (3) (2 m only). - Gray Level Co-occurrence Matrix (GLCM): mean, variance, homogeneity, contrast, dissimilarity, entropy, angular second moment, and correlation (8) Gray Level Difference Vector (GLDV): mean, variance, entropy, angular second moment, and contract (5) - Sum and Difference Histogram (SADH): mean, variance, homogeneity, contrast, energy, entropy, and correlation (7)	20 for texture-12m 23 for texture-2m
Multi-angle view (MA) variables	Reflectance	Surface reflectance at 5 DMC angles	20
	BRDF	- Re-constructed hot spot (4 bands) and dark spot (4 bands) reflectance data - Hotspot and dark-spot index (HDS) (4 bands) - Normalized difference between hotspot and dark-spot (NDHD) (4 bands)	16

6. Overview of Chinese YSs research

Model	Variables	R^2	RMSE (t/ha)
RF	NV reflectance	0.38±0.03	13.12±0.53
	NV reflectance + Texture-12m	0.38±0.03	13.29±0.43
	NV reflectance + Texture-2m	0.42±0.02	12.71±0.46
	MA reflectance	0.53±0.05	11.74±0.55
	MA reflectance + Texture-12m	0.54±0.02	11.04±0.40
	MA reflectance + Texture-2m	0.59±0.02	11.21±0.49
	MA reflectance + BRDF	0.60±0.03	10.86±0.53
	MA reflectance + BRDF+ Texture-12m	0.60±0.03	10.90±0.49
	MA reflectance + BRDF + Texture-2m	**0.61±0.02**	**10.31±0.33**
DNN	NV reflectance	0.40±0.02	12.81±0.49
	NV reflectance + Texture-12m	0.40±0.03	12.75±0.50
	NV reflectance + Texture-2m	0.45±0.02	12.42±0.43
	MA reflectance	0.56±0.02	11.23±0.27
	MA reflectance + Texture-12m	0.57±0.02	11.28±0.56
	MA reflectance + Texture-2m	0.60±0.02	10.56±0.42
	MA reflectance + BRDF	0.62±0.03	10.61±0.30
	MA reflectance + BRDF + Texture-12m	0.60±0.02	10.85±0.29
	MA reflectance + BRDF + Texture-2m	**0.65±0.03**	**10.24±0.41**

6. Overview of Chinese YSs research

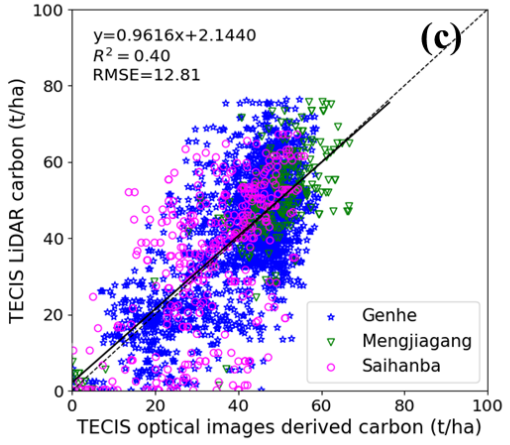


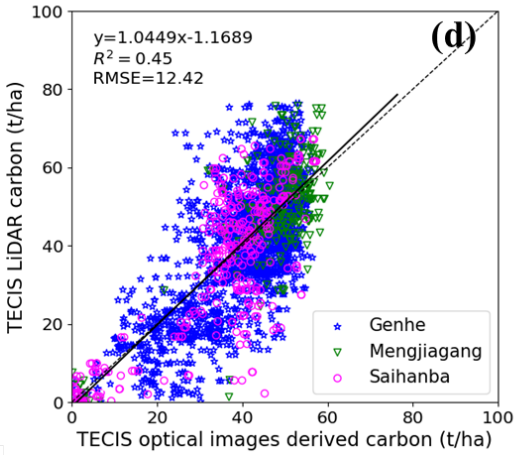


Cross validation accuracy of RF based on Nadir variables

(a)Ref

(b)Ref+texture-2m





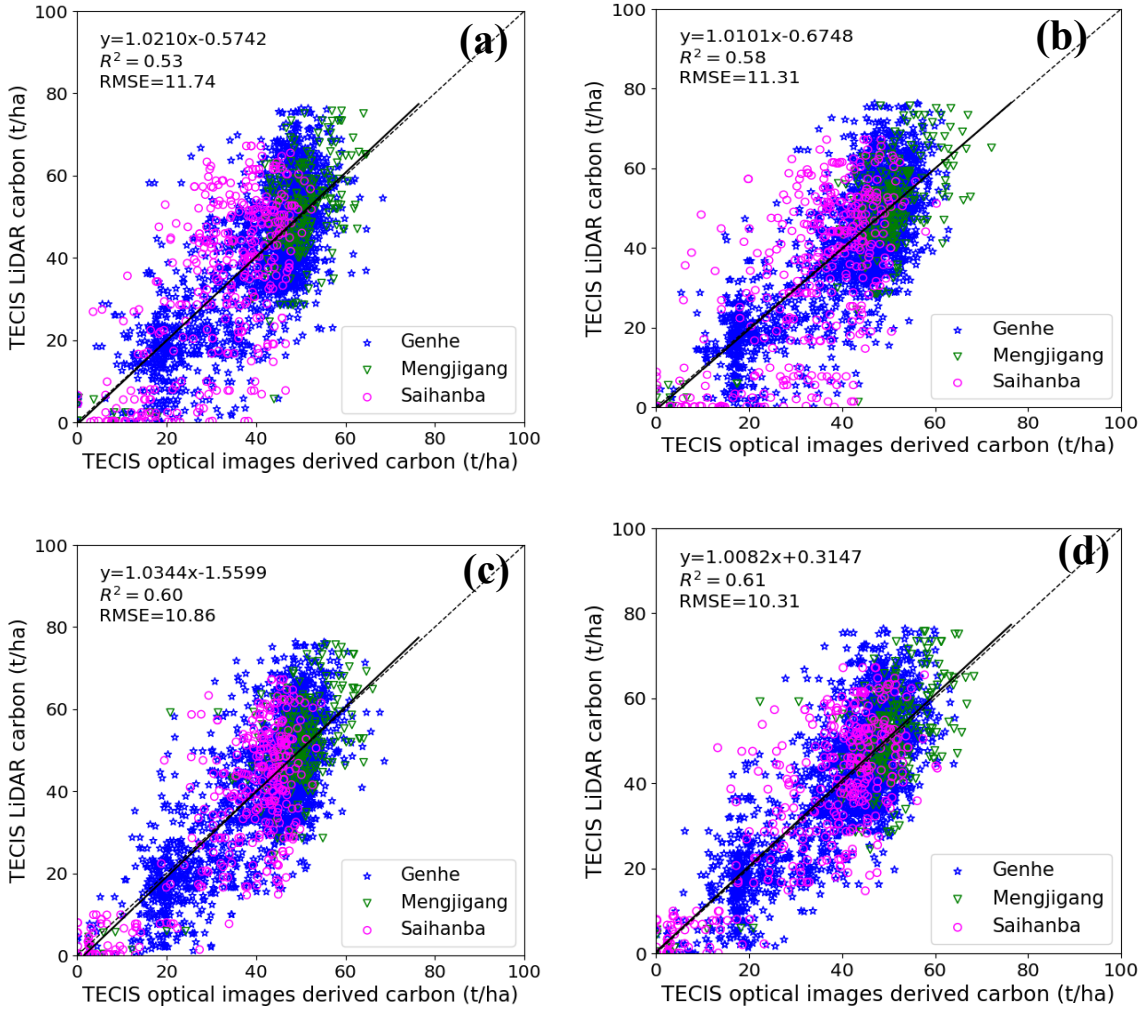
Cross validation accuracy of DNN based on Nadir variables

(c)Ref

(d)Ref+texture-2m

When using single-angle variables, forest carbon was overestimated in the low-value and underestimated in the high-value.

6. Overview of Chinese YSs research



Cross validation accuracy of RF based on multiple angle variables

(a) Ref

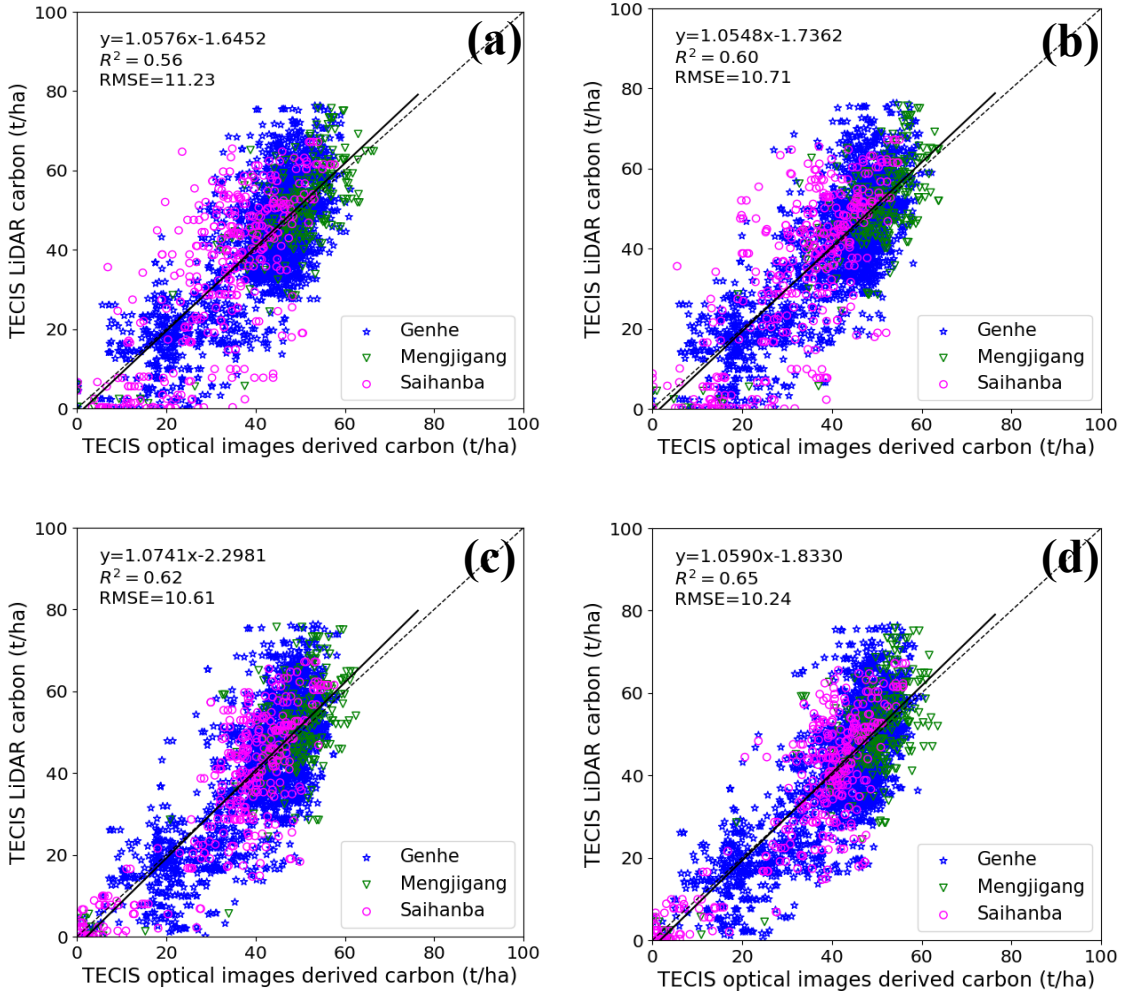
(b) Ref + texture-2m

(c) Ref + BRDF

(d) Ref + BRDF + texture-2m

BRDF and texture information improve the accuracy of forest carbon estimation.

6. Overview of Chinese YSs research



Cross validation accuracy of DNN based on multiple angle variables

(a) Ref

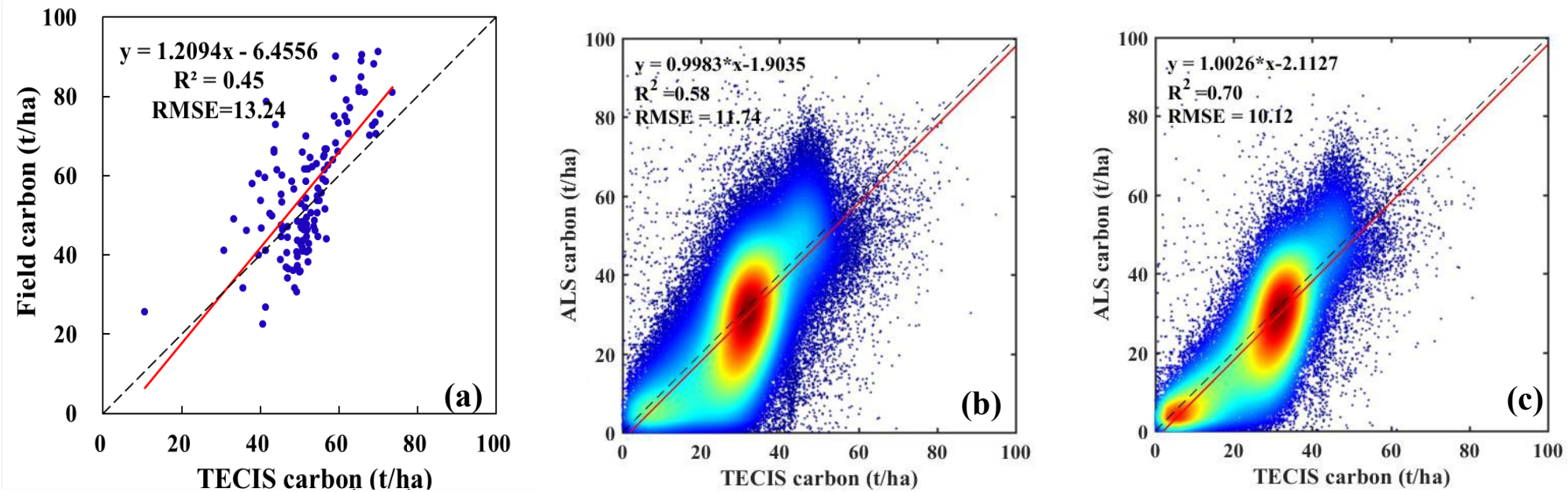
(b) Ref + texture-2m

(c) Ref + BRDF

(d) Ref + BRDF + texture-2m

BRDF and texture information improve the accuracy of forest carbon estimation.

6. Overview of Chinese YSs research



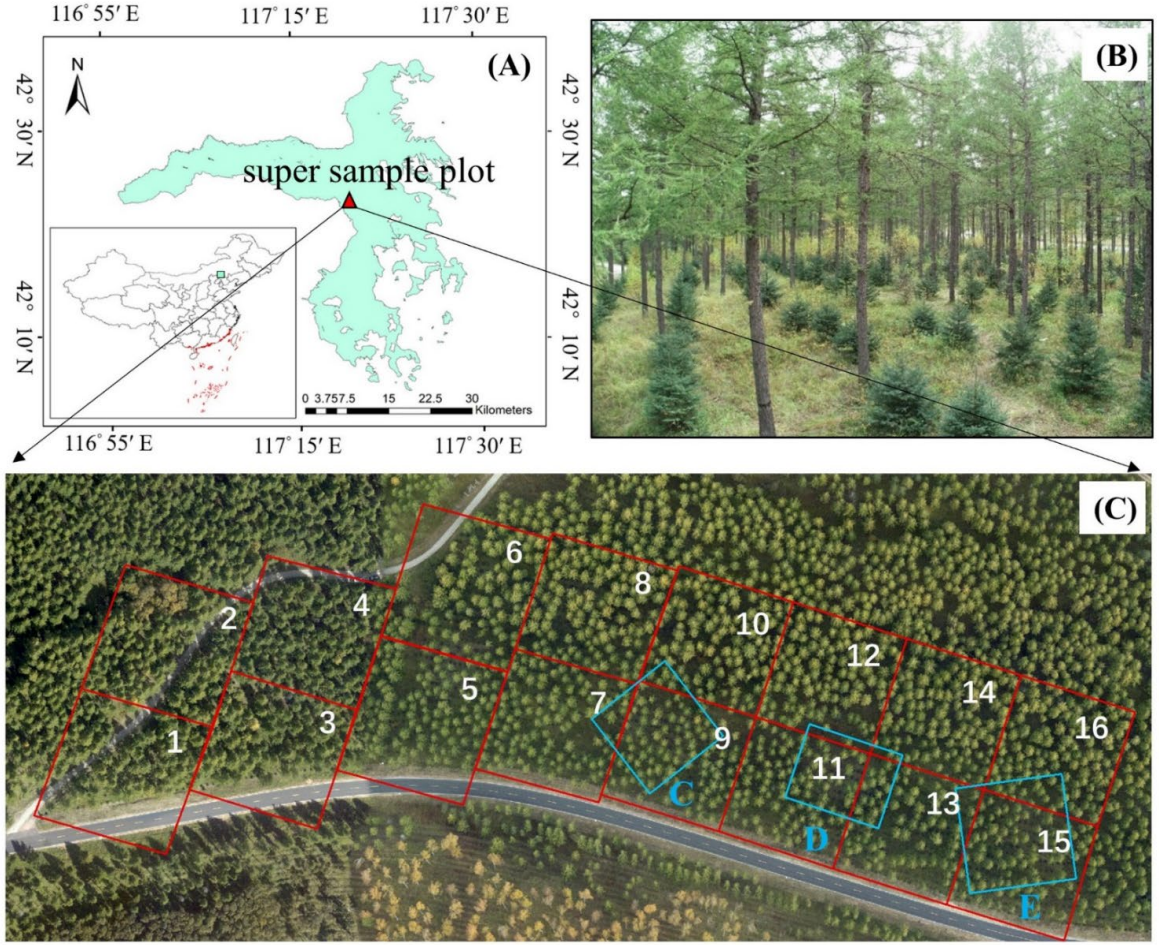
Assessment of ACD maps derived through CASAL-DMC integration using field plot data (a) and ALS-based carbon estimates at the 25m (b) and 100m (c) resolutions.

Conclusion

- Multiple angle optical observations on TECIS have some advantages in wall to wall forest carbon estimation.
- BRDF information and texture enhances the forest carbon estimation capability.

6. Overview of Chinese YSs research

2. Identifying regenerated saplings by stratifying forest overstory using airborne LiDAR data



Study area and data

Tree species：

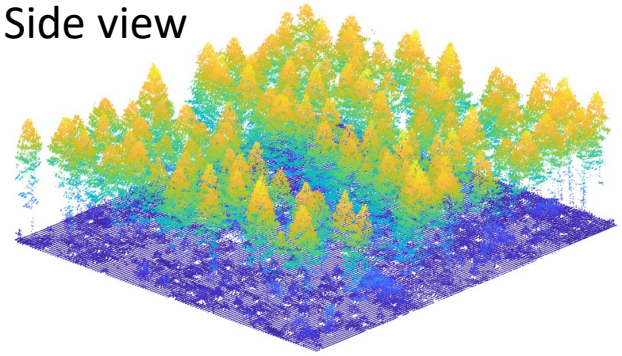
The sample plot is a two-layered forest, with the upper layer consisting of mature larch trees and the lower layer comprising young spruce trees.

Data：

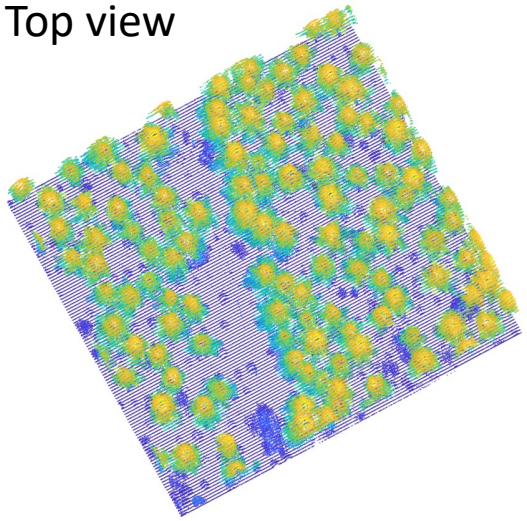
- Airborne LiDAR data acquired in September 2018 using the CAF-LiCHy system（red）
- Point density is 243pts/m^2
- Field-measured data collected in August 2017
- Terrestrial LiDAR data acquired in September 2018.（blue）

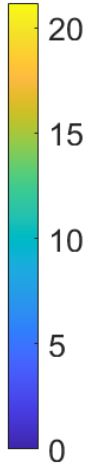
6. Overview of Chinese YSs research

Side view

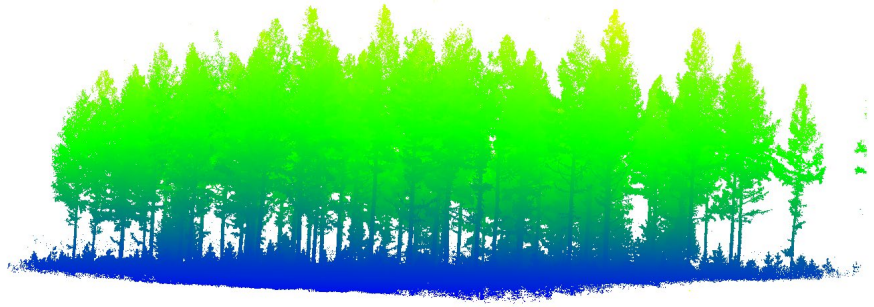


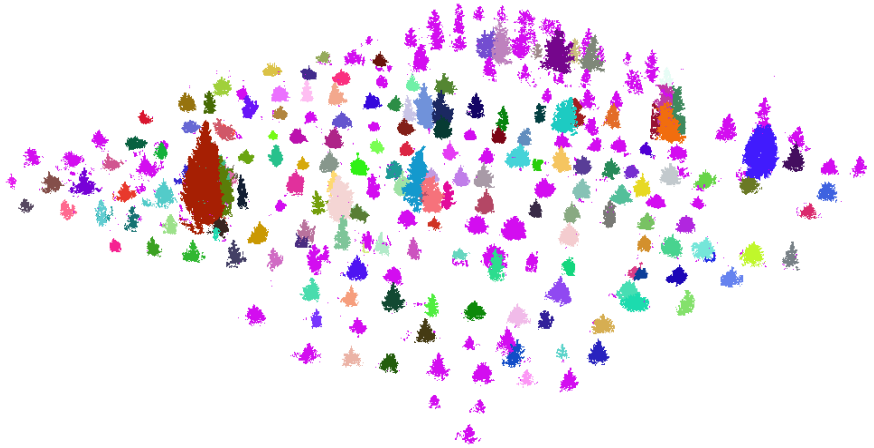
Top view





ALS data





TLS verification data



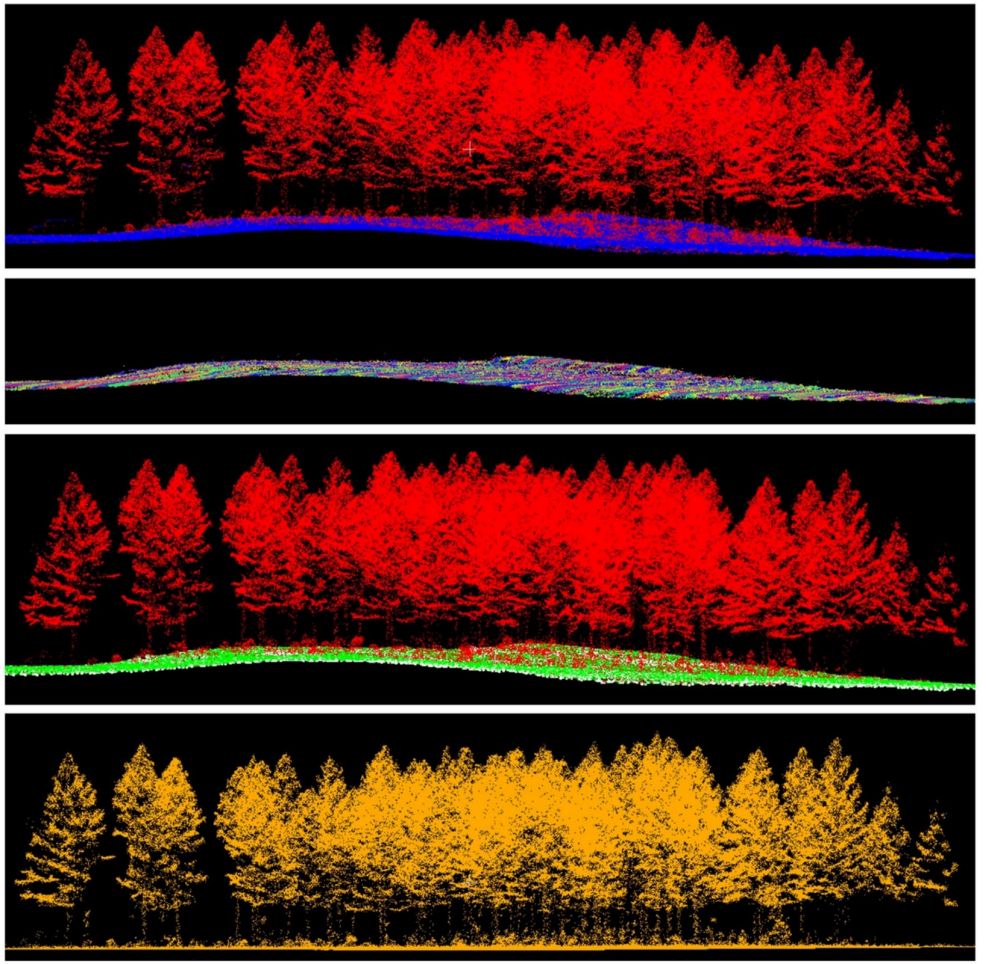


Field measurement

6. Overview of Chinese YSs research

Methods

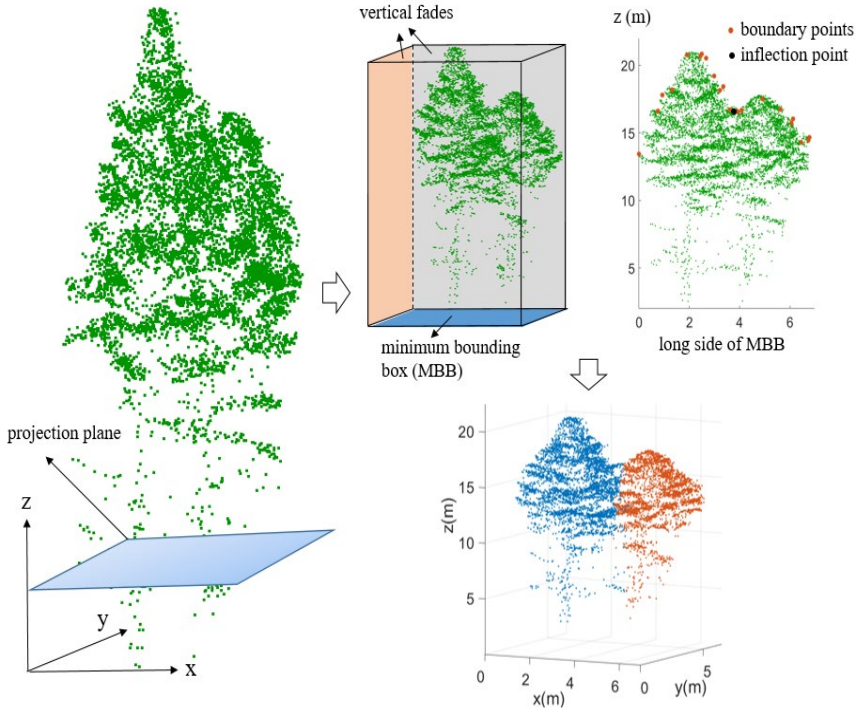
To address the issue that existing point cloud filtering algorithms fail to effectively remove near-ground noise (such as weeds), leading to large errors in tree height estimation-particularly for understory saplings-an optimized point cloud filtering method based on regular voxels is proposed.



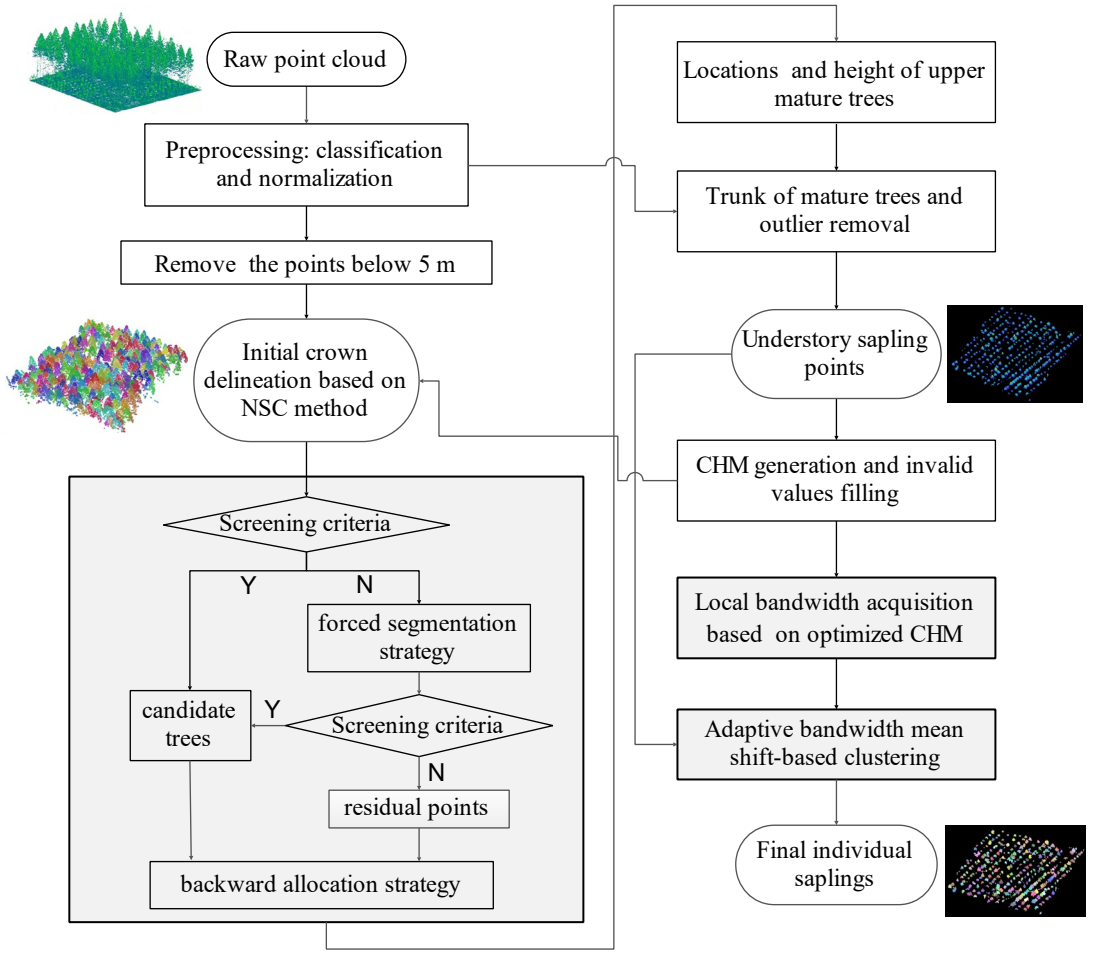
Fine normalization: (A) CSF point cloud filtering; (B) Voxelization of initial ground points; (C) Separation of true ground points and pseudo-ground points; (D) Point cloud normalization.

6. Overview of Chinese YSs research

- Upper-layer large tree segmentation based on NSC
- Post-processing of individual tree segmentation considering crown structure.
- Adaptive Kernel Bandwidth Mean-Shift Sapling Segmentation

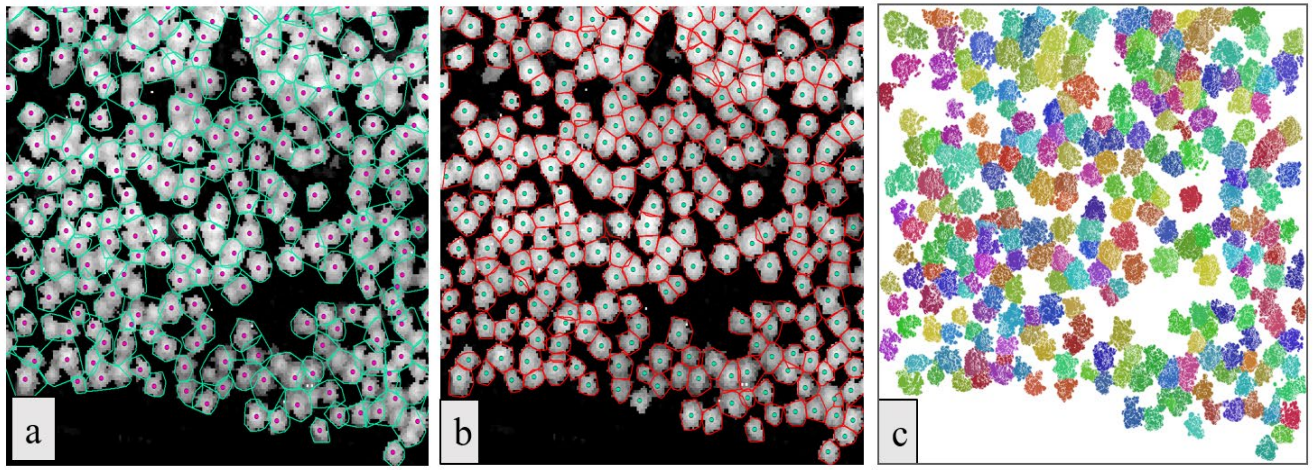


Post-processing of individual tree segmentation using NSC.

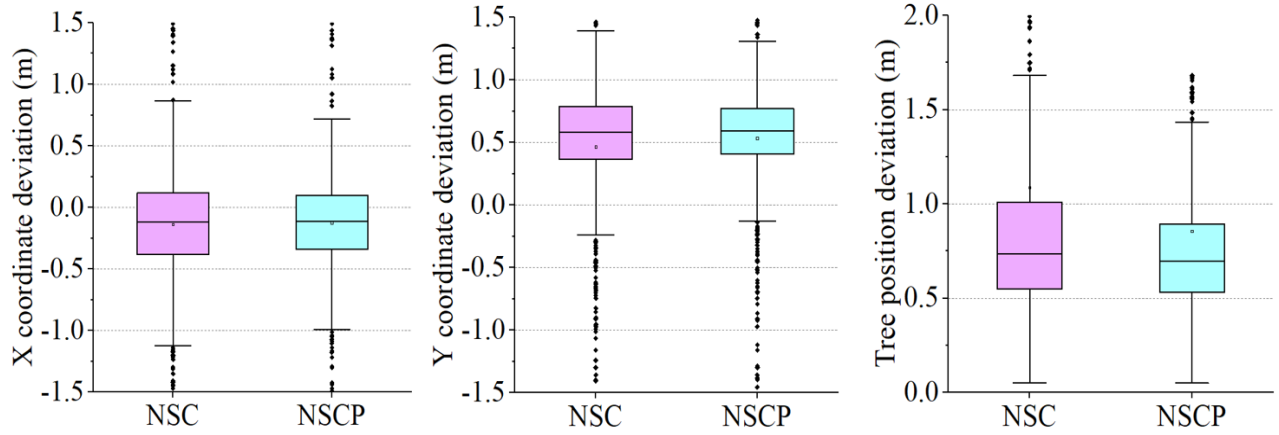


Method flowchart: the left side shows the segmentation process for upper-layer large trees, while the right side illustrates the segmentation process for lower-layer saplings.

6. Overview of Chinese YSs research



Comparison of individual tree segmentation results before and after optimization: (a) overlay of canopy boundaries and CHM before optimization; (b) overlay of canopy boundaries and CHM after optimization; (c) top view of the point cloud segmentation results after optimization.



Trunk position detection error before and after post-processing

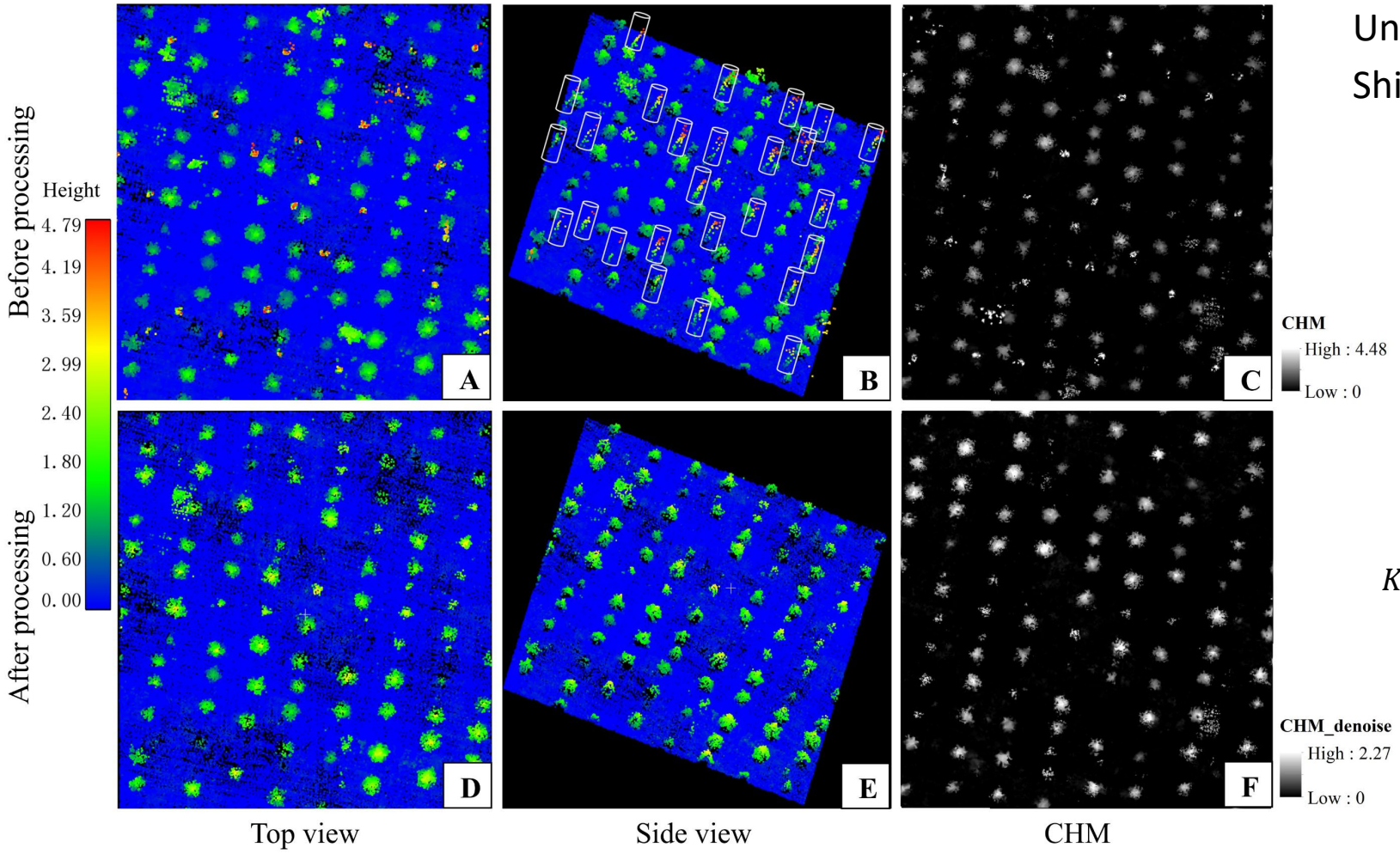
NSCP results:

- The upper canopy boundaries are more distinct
- The error in the location of the upper trunk compared to the measured individual tree position has decreased

Remove the following points:

- point cloud of large tree canopies
- trunk points of large trees mixed among small trees

6. Overview of Chinese YSs research



Removal of upper-level point clouds and generation of sapling canopy height model

Understory Sapling Segmentation Using Mean-Shift with Adaptive Kernel Bandwidth

- Initial crown size of small trees and their distance to neighbors

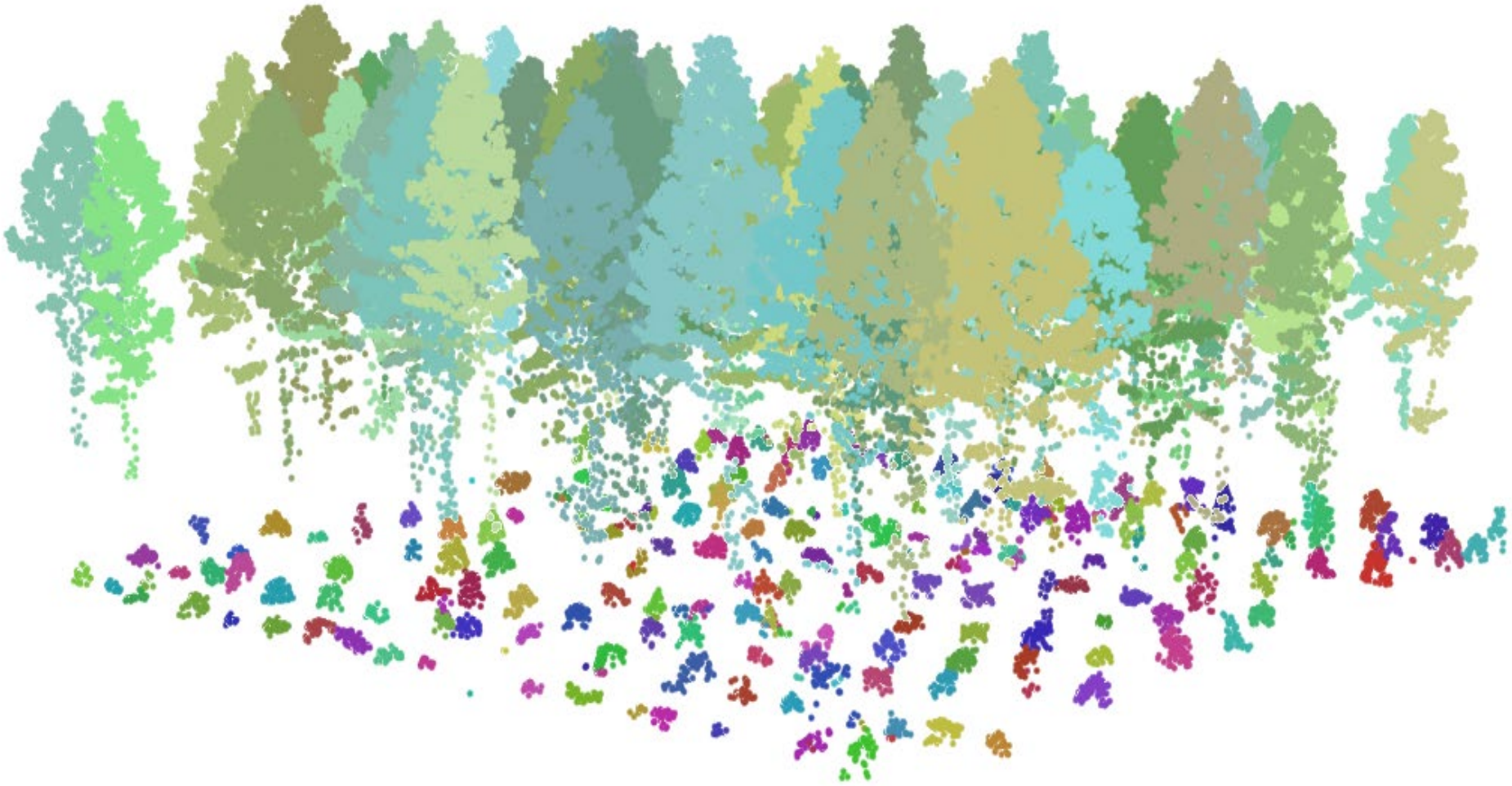
$$h_{loc}^{m} = \frac{\partial \times radius_m}{\mu \times sd_m}$$

input

$$K\left(\left\|\frac{x_0 - x_i}{h}\right\|^2\right) = \begin{cases} exp\left(-\frac{1}{2}\left\|\frac{x_0 - x_i}{h}\right\|^2\right) & if \ \left\|\frac{x_0 - x_i}{h}\right\|^2 \le 1 \\ 0 & otherwise \end{cases}$$

$$x_0 \leftarrow \frac{\sum_{i=1}^{n} x_i K\left(\left\|\frac{x_0 - x_i}{h}\right\|^2\right)}{\sum_{i=1}^{n} K\left(\left\|\frac{x_0 - x_i}{h}\right\|^2\right)}$$

6. Overview of Chinese YSs research



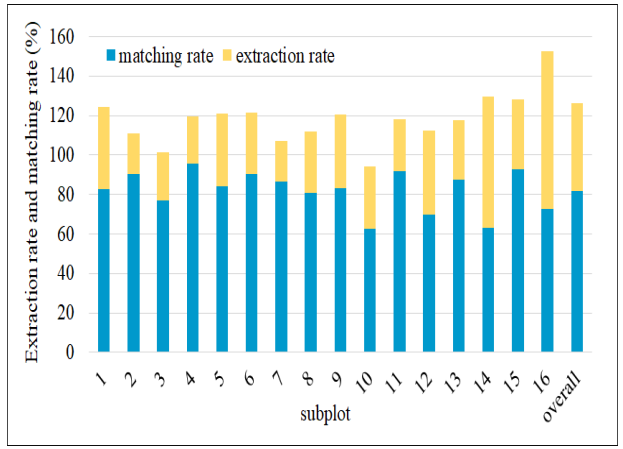
Segmentation results of overstory trees and understory saplings

6. Overview of Chinese YSs research

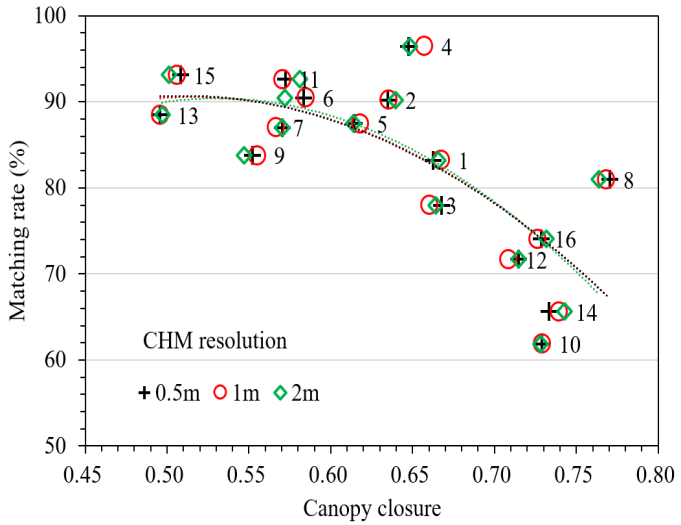
- Extraction rate is affected by noise from understory shrubs and grasses；
- Areas with relatively large overstory gaps and sparse understory shrubs can achieve higher matching rates.

  Extraction rate： 94.41% - 152.78% (126.37%)

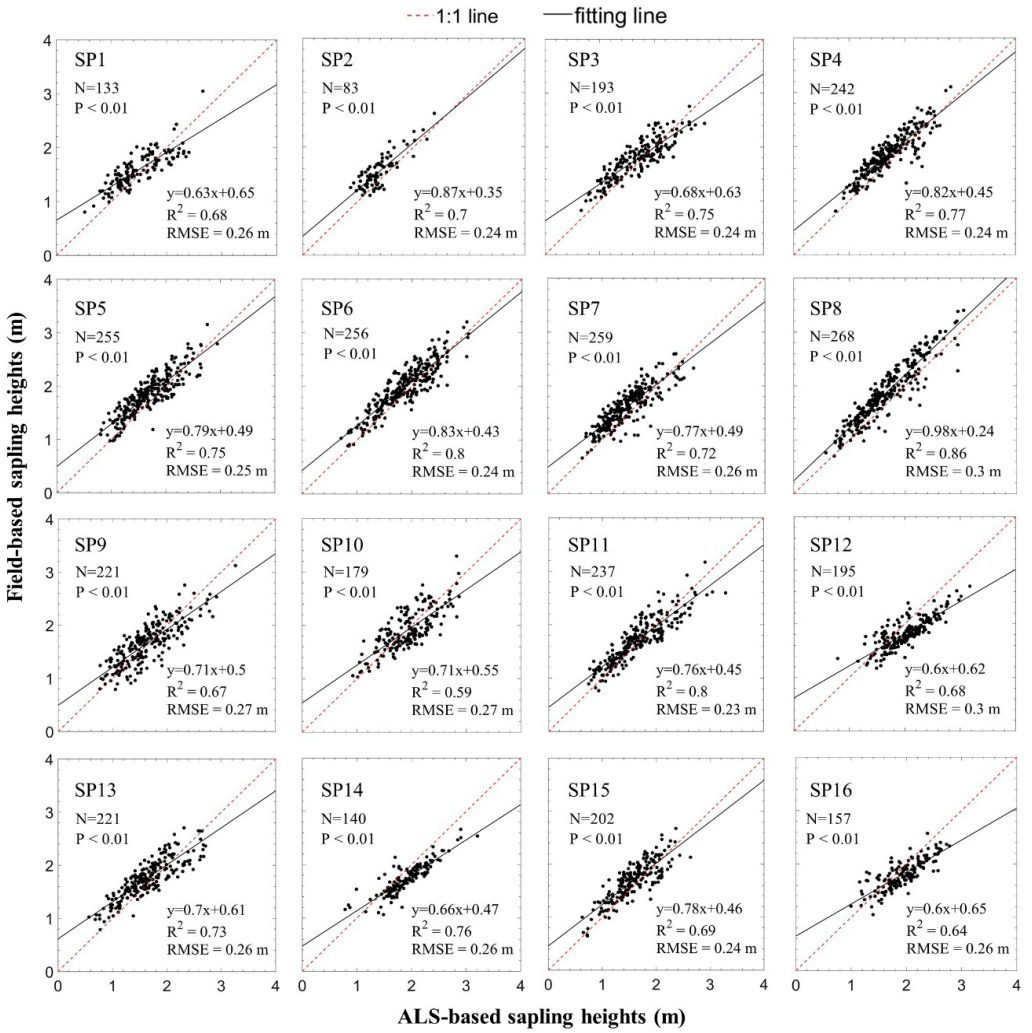
  Matching rate： 62.59% - 95.65% (81.78%)
- The R^2 values for the tree heights range from 0.59 to 0.86, with RMSE between 0.23 m and 0.3 m.
- The matching rate decreases as canopy closure increases



Extraction and matching rate



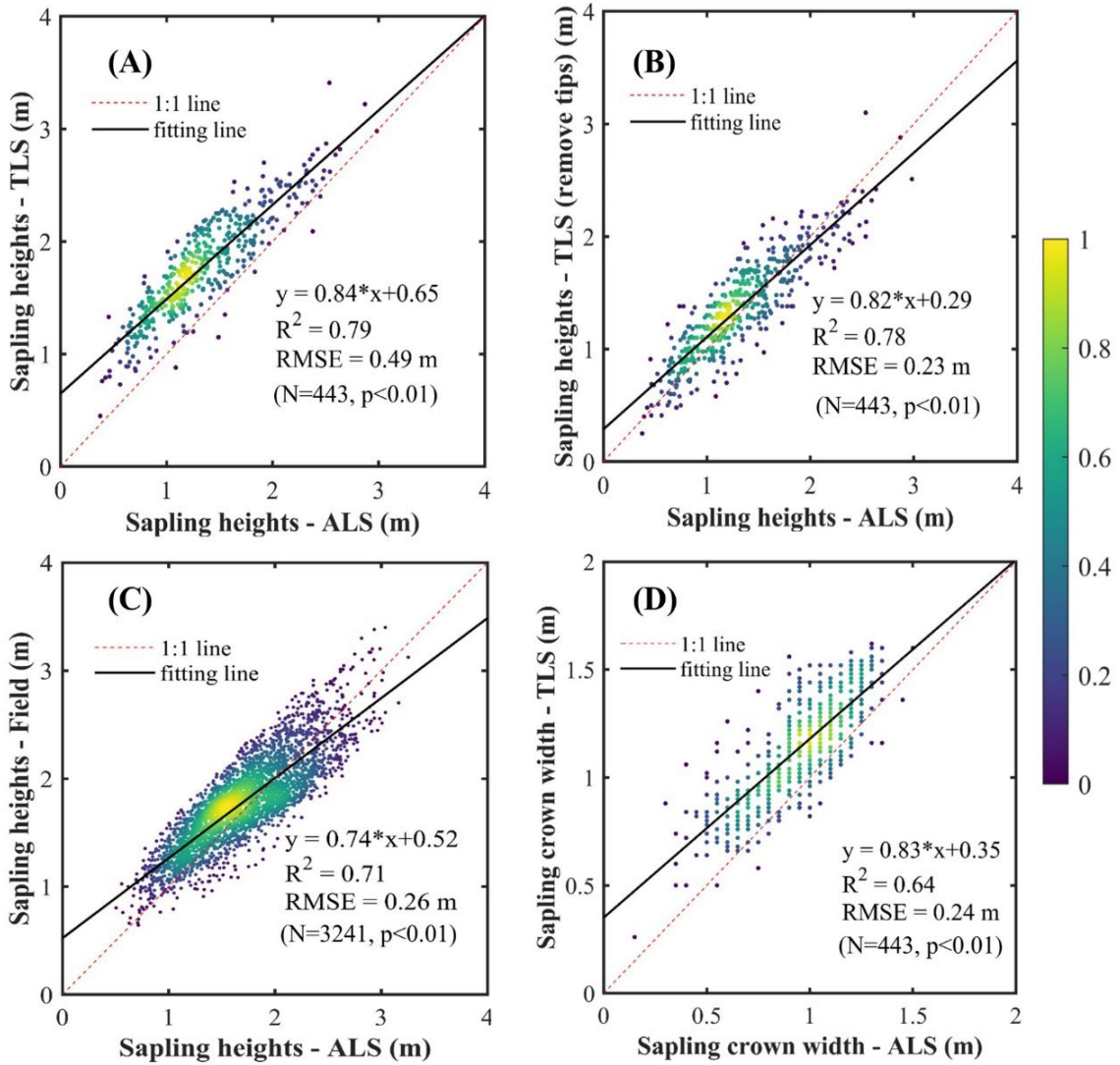
Relationship between Matching Rate and Overstory Canopy Closure



Comparison of Segmented Sapling Heights with Measured Heights

6. Overview of Chinese YSs research

- Sapling heights extracted from ALS show a strong correlation with field-measured values and TLS measurements.
- ALS can detect the tree height of saplings but has difficulty detecting the treetop sections.
- Due to occlusion, ALS struggles to fully capture the sapling crowns, resulting in an underestimation of crown size, especially for smaller crowns.

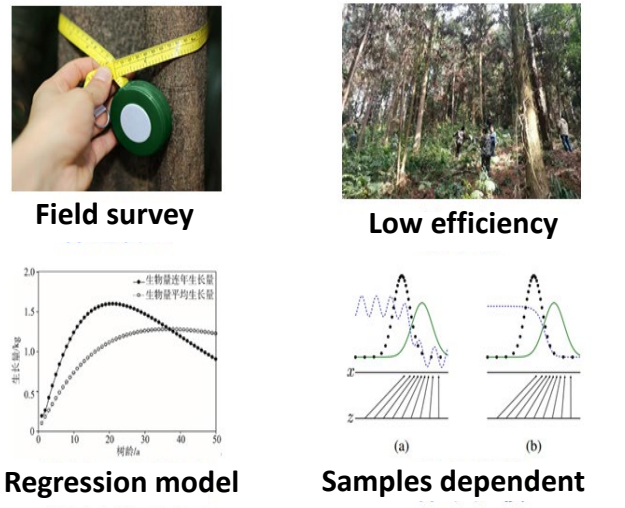


Comparison with TLS and field data and the Validation of canopy results

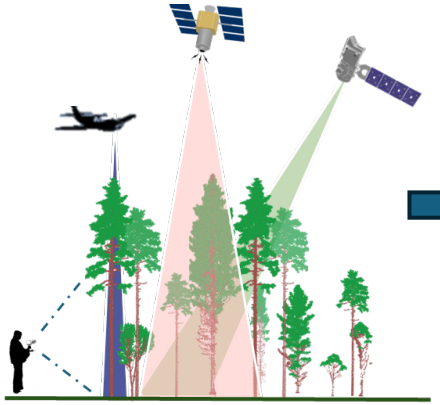
6. Overview of Chinese YSs research

3. Aerial LiDAR is All You Need for Regional Forest Biomass Mapping: Progressively Synergizing Individual-tree and Area-based Approaches

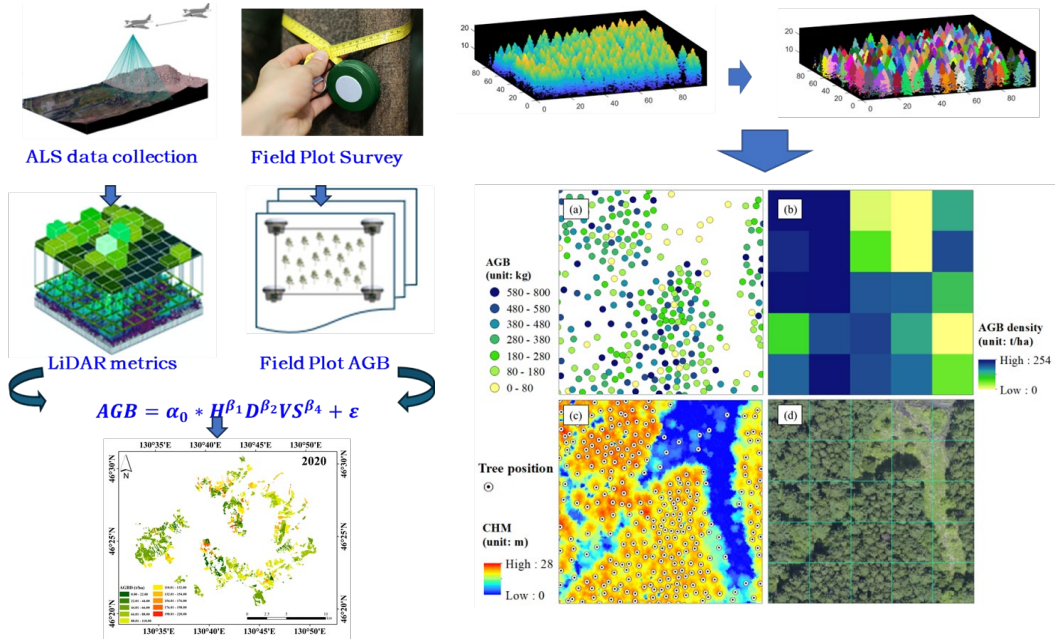
- **Direct 3D Forest Structure Measurement: The Key to High-Precision Biomass Retrieval**
- **Traditional methods struggle to perform measurements over large areas.**
- **LiDAR can rapidly acquire data across extensive regions, but the modeling process remains sample-dependent.**
- **This reliance on samples limits further methodological development.**



Traditional methods



Multi-platform LiDAR Observation System

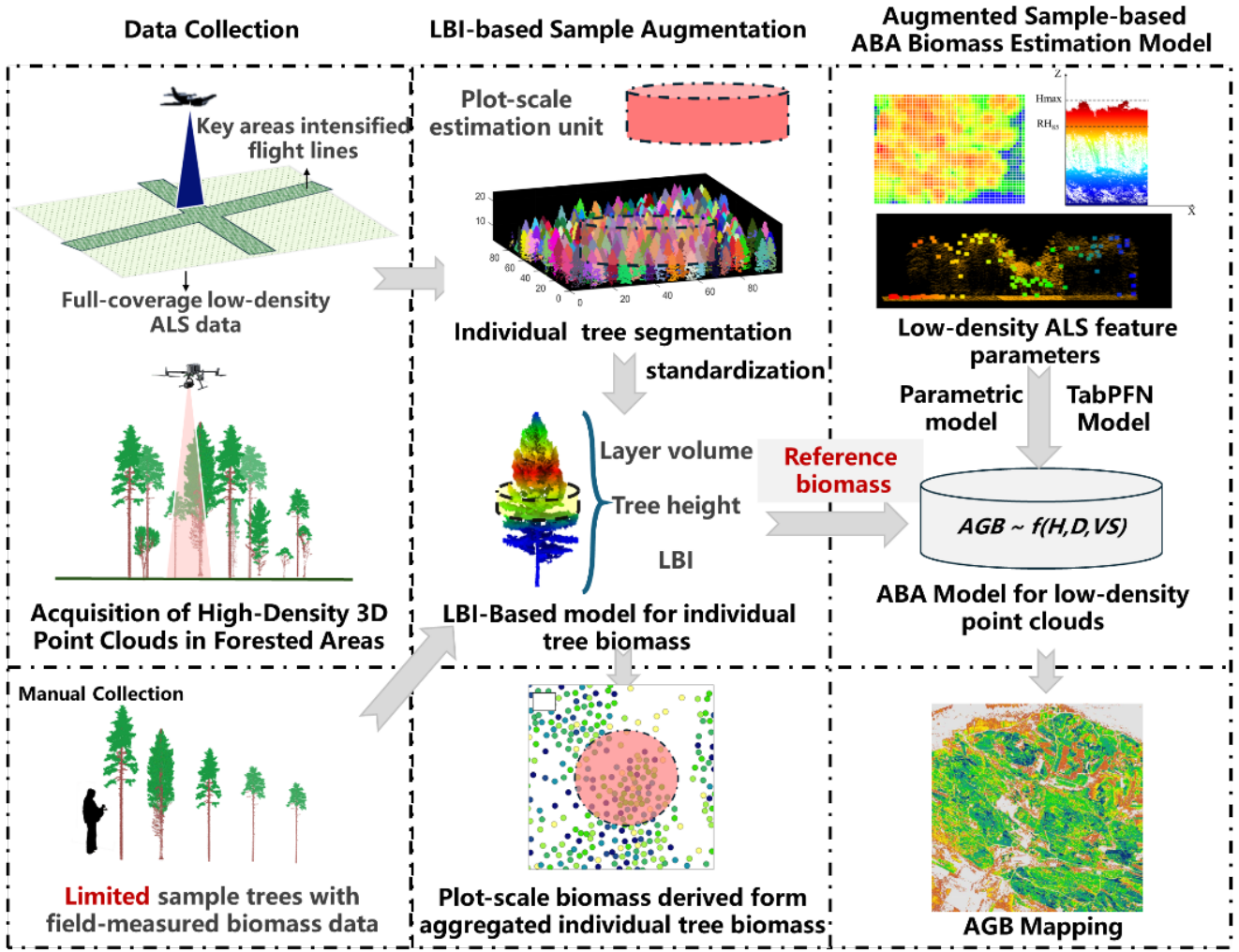


Sample dependency in LiDAR-based approaches

(Coops et al.,2021; Dwiputra et al.,2023; Duncanson et al. 2022)

6. Overview of Chinese YSs research

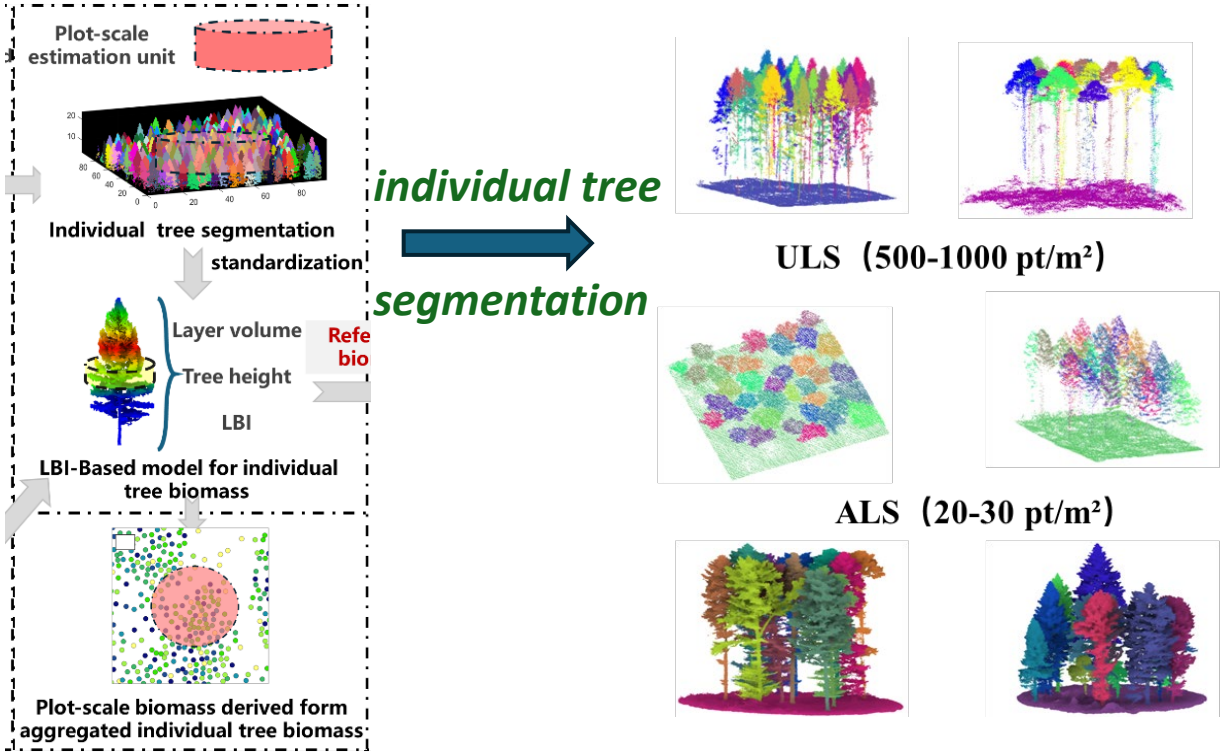
- *High-Density Aerial LiDAR* as a Substitute for Field-Plot Sampling
- Reduce manual field-plot surveys by *90%+*

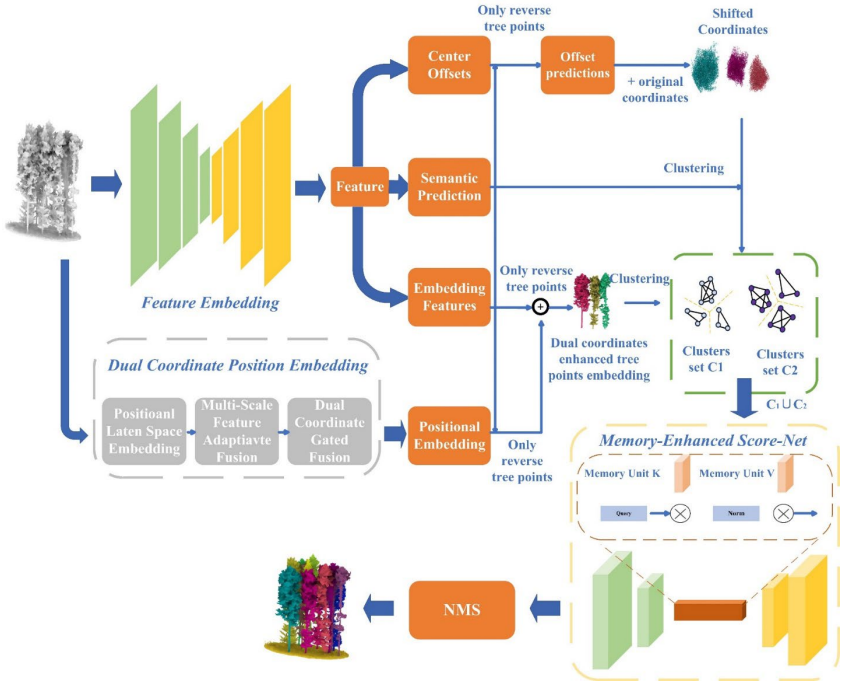


- This approach leverages the LBI method to derive high-precision *stand-level biomass* from *high-density Aerial point clouds* as a substitute for field plot data.
- Initially, precise *individual-tree segmentation* is conducted on high-density aerial LiDAR data.
- Combined with a limited set of field-measured tree parameters, an *individual-tree-level biomass model* is then established.
- Subsequently, *plot-scale biomass* accumulation is carried out according to a tailored tree selection strategy.
- Lastly, the resultant biomass data are matched with feature parameters extracted from low-density point cloud data to develop a biomass estimation model based on ABA, ultimately enabling *large-scale forest biomass* estimation and mapping.

6. Overview of Chinese YSs research

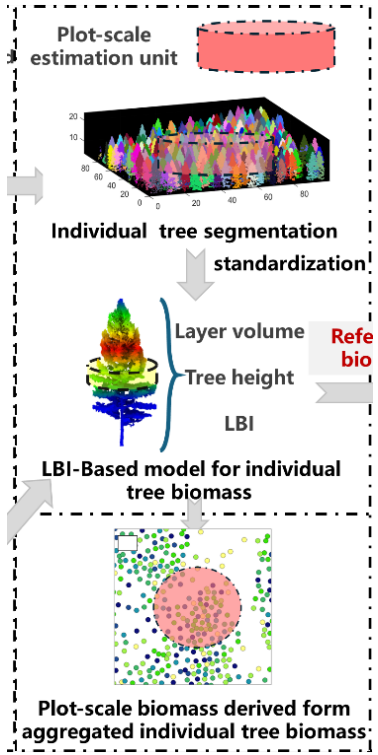
- Accurate *individual tree* point cloud *segmentation* is crucial for biomass estimation and sample augmentation.
- This study utilizes a deep learning-driven end-to-end segmentation network, ITS-Net (Individual Tree Segmentation Network).
- ITS-Net, trained on multi-source datasets covering *various forest types* and aerial platforms, incorporates *global-view features* and *dual coordinate multi-scale positional embeddings* to guide the network towards precise segmentation, providing detailed point cloud data for each tree





6. Overview of Chinese YSs research

- A highly accurate and universally applicable individual-tree biomass estimation model is the cornerstone for generating augmented biomass samples.
- We propose the LiDAR Biomass Index (LBI), an individual-tree biomass estimation approach optimized for aerial LiDAR data.



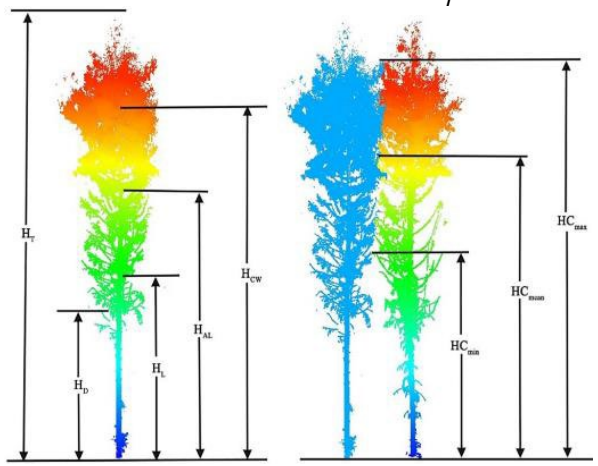
Canopy Index as a Substitute for DBH

individual tree segmentation

$$AGB = F \cdot \rho^{\beta} \cdot \pi^{\beta} \cdot H_T^{\beta} \left(\frac{1}{4}D^2\right)^{\beta} \qquad D^{\alpha} \propto \sum_{H_c}^{H_T} Cover(H) \cdot H$$

$$LBI = \lim_{\Delta H \to 0} \sum_{H=H_c}^{H_T} U_L(H) \cdot [r(H)]^2 \cdot \Delta H \cdot H$$

$$AGB = aLBI^{b} H_T^{\ c}$$

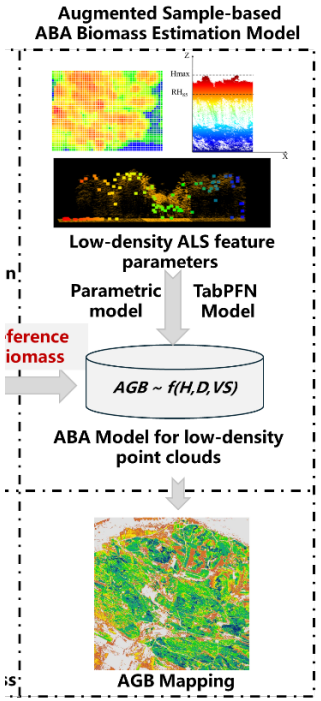


This method has been incorporated into China's Voluntary Greenhouse-Gas Emission-Reduction Project Methodology: Afforestation Carbon Sequestration (CCER-14-001-V01).

6. Overview of Chinese YSs research

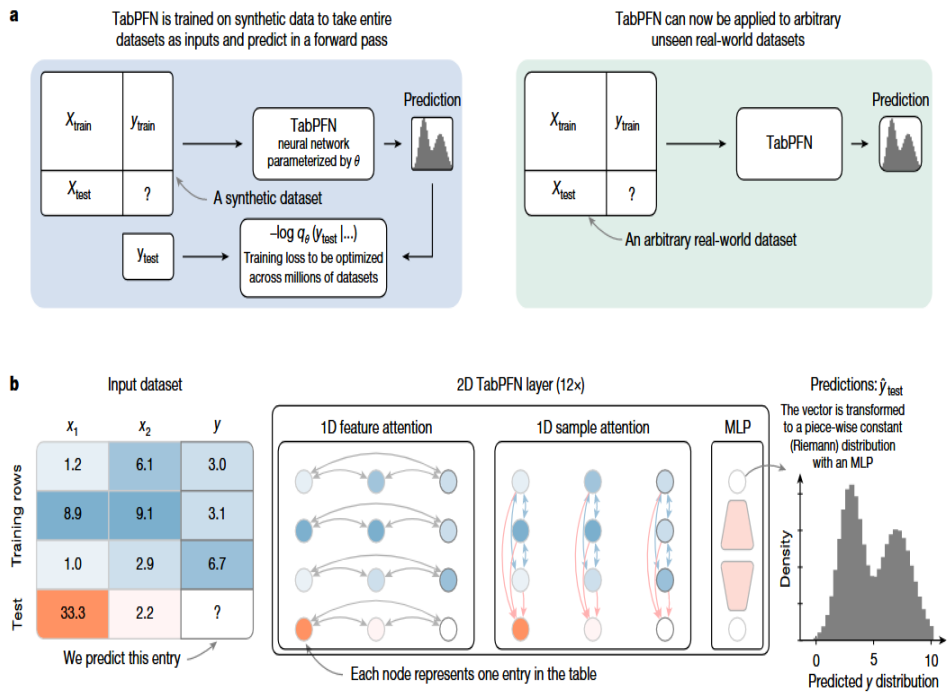
- **Accordingly, to fully exploit the available feature information and minimize cumulative errors across different models, we introduce a small-sample deep-learning biomass estimation framework： *TabPFN***

Low-density point clouds ⟷ **ABA Model** ⟷ **Biomass of augmented-sample**



LiDAR Features	Description	Reference
Rh_5, Rh_{10}…, Rh_{98}	Relative Height percentiles of the canopy point cloud, indicating the elevations at which 5th, 10th, … 95th of vegetation points are distributed.	Roussel et al., 2020
$Height_{mean, var, cv, skewness}$	Statistical metrics derived from the vertical distribution of point clouds, such as mean, variance, coefficient of variation, skewness, and related descriptors.	
$H_{zabovezmean}$	Fraction of points that exceed the mean canopy height.	
TCH	Mean height of the uppermost canopy layer.	Du et al., 2023
MCH	Average height of the canopy profile.	Asner et al., 2012
LAVH	Height weighted by Leaf Area Index.	Asner et al., 2014
Rumple of CHM	Ratio of the canopy's outer surface area to the ground surface area, with higher rumple values reflecting increased vertical and horizontal structural complexity.	Almeida et al., 2019

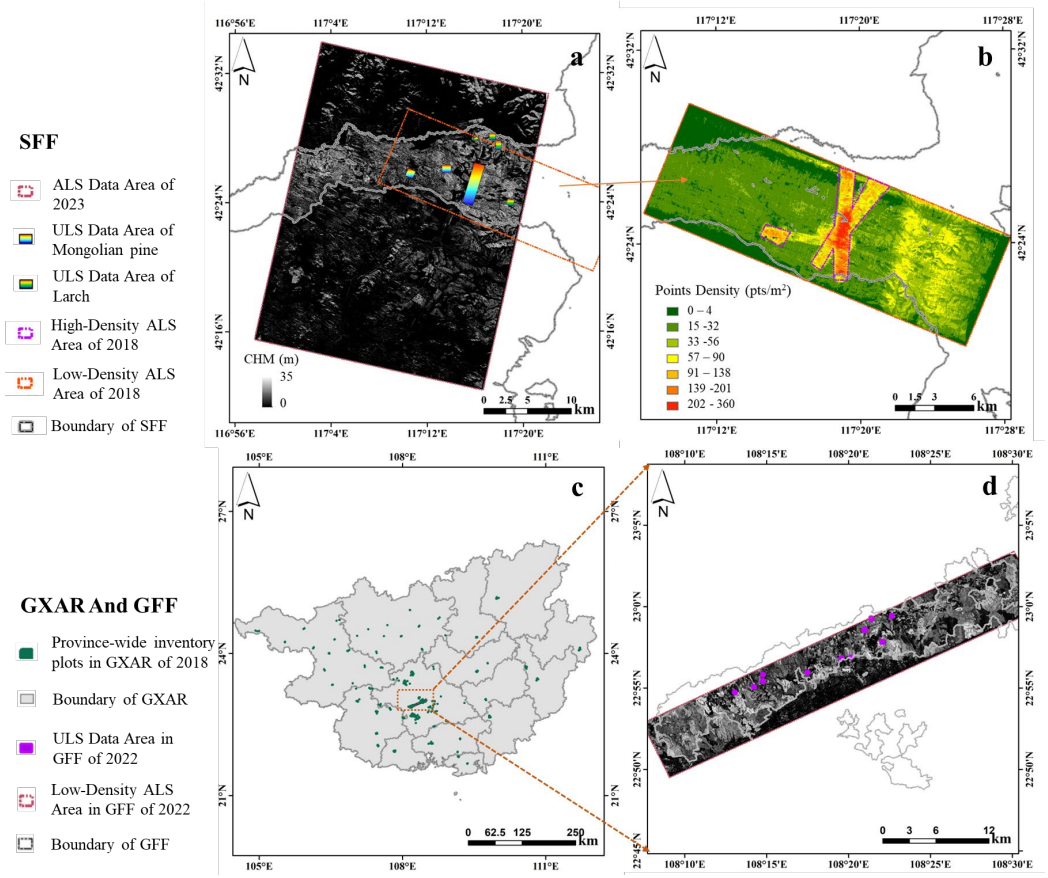
LiDAR Features and Descriptions for ITS-ABA and ABA Model to estimate AGB using low-density LiDAR



(Hollmann et al.,2025)

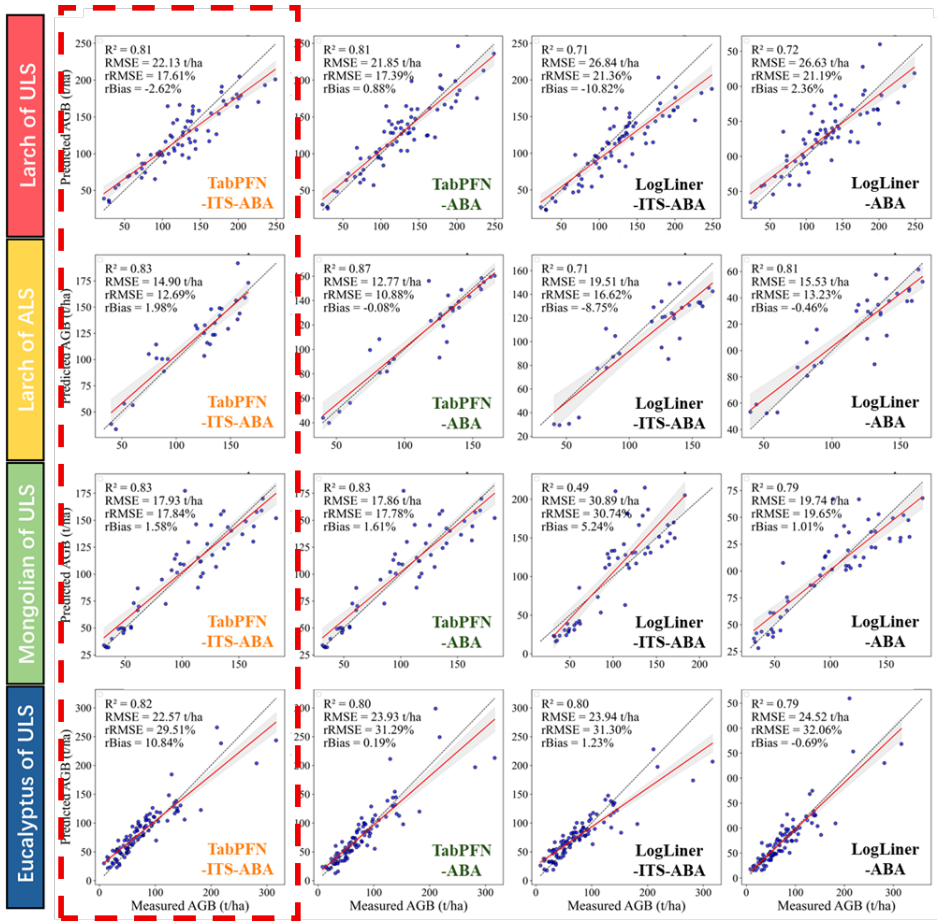
6. Overview of Chinese YSs research

Multi-Platform Plot-Scale Accuracy



In northern China, at Saihanba Forest Farm (SFF).
In southern China, at Gaofeng Forest Farm (GFF) near Nanning, Guangxi (local high-density point clouds) and Guangxi Zhuang Autonomous Region (GXAR).

Zero Field Plots, Enhanced Accuracy!



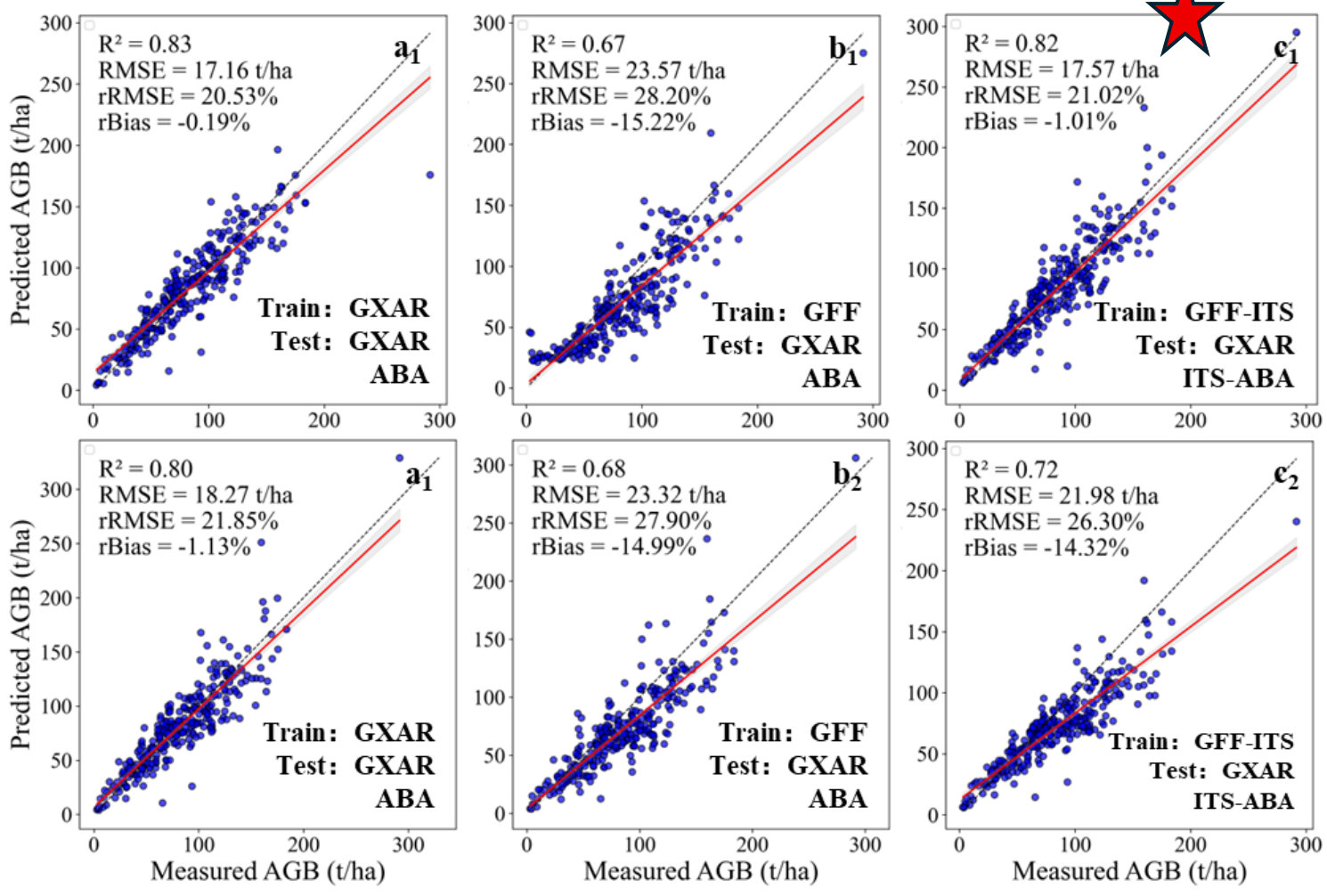
Validation accuracy of biomass estimation models developed from augmented and actual plot samples

6. Overview of Chinese YSs research

Regional transferability of the ITS-ABA model for the province level

TabPFN

LogLiner



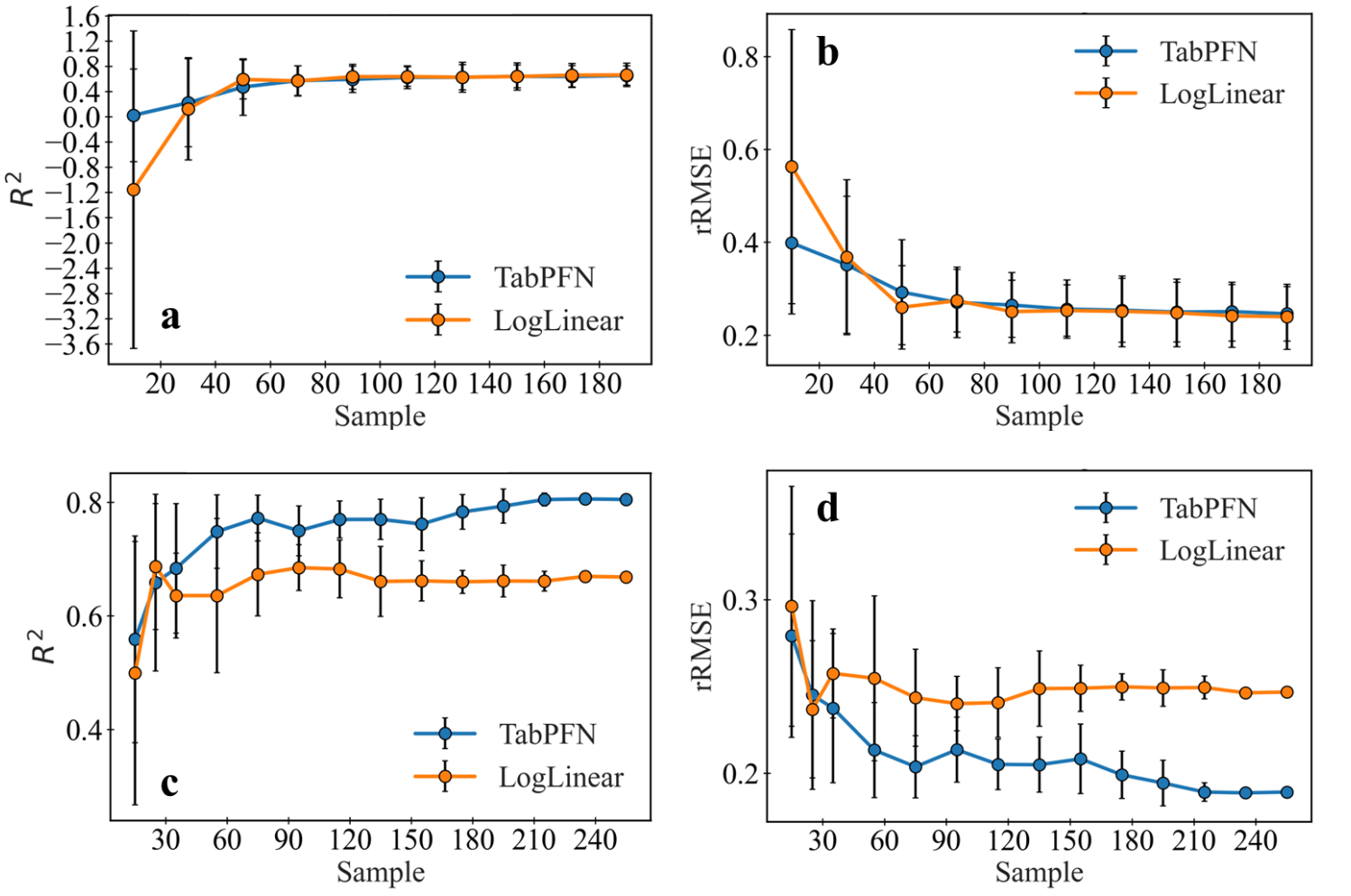
- The ITS–ABA model exhibits ***superior transferability***.
- The ITS–ABA workflow produces a ***more balanced sample distribution***, especially for high-biomass classes.

6. Overview of Chinese YSs research

- **Effect of sample size on model accuracy.**

Augmented plots

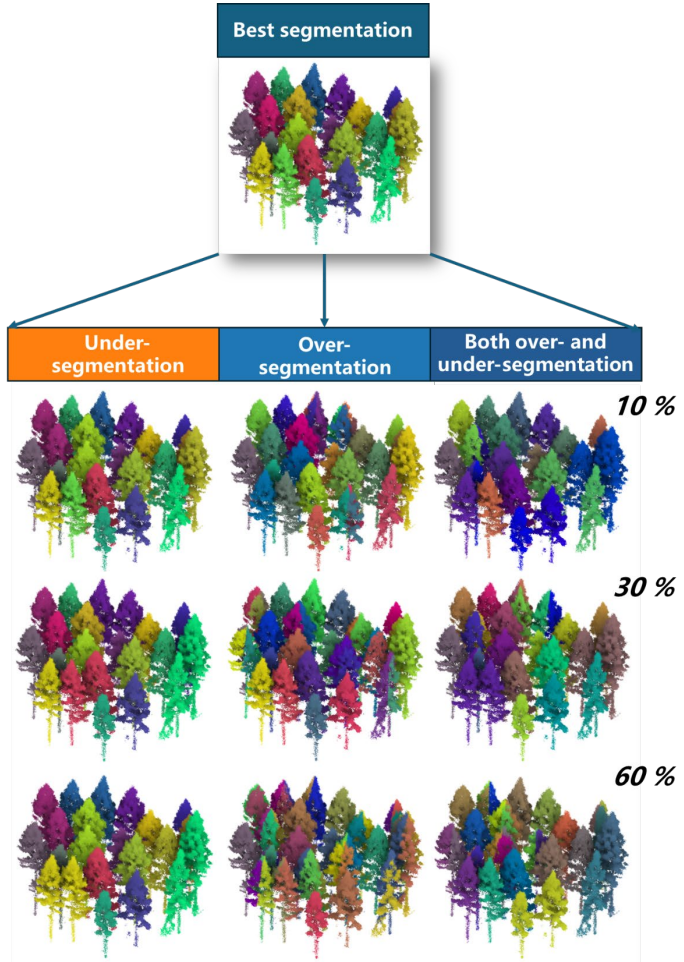
Individual-tree samples



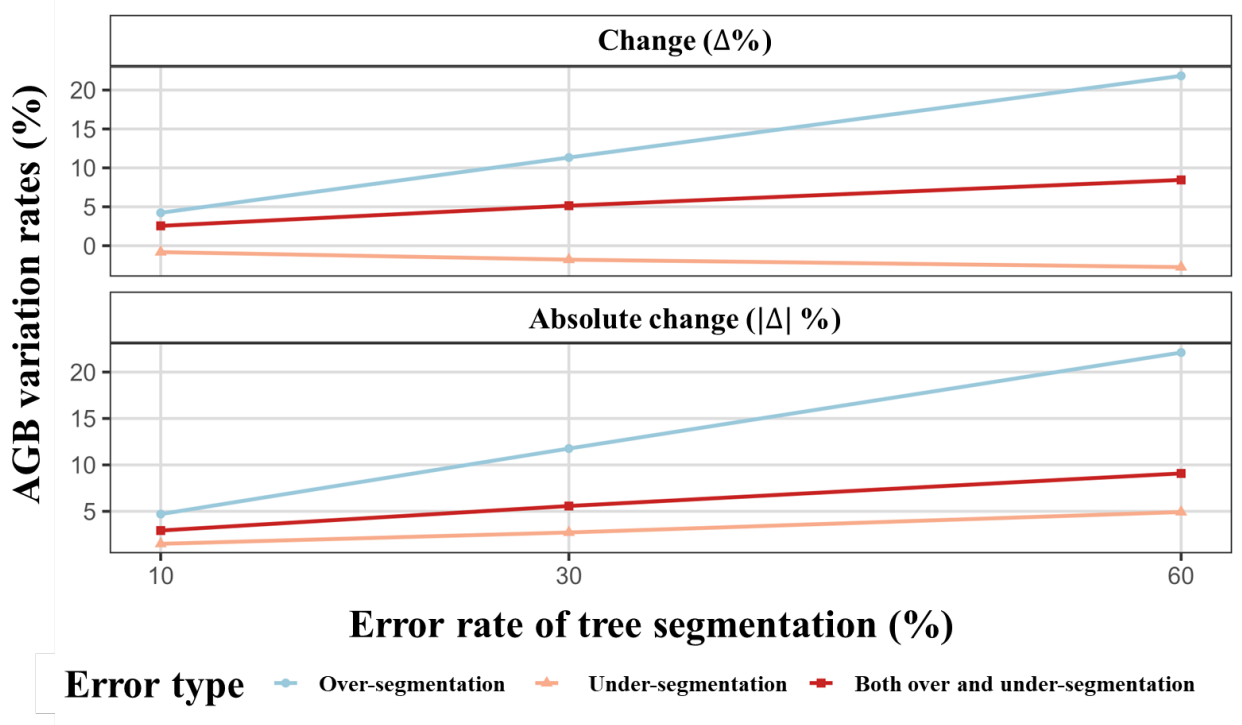
- For our biomass-estimation model, accuracy plateaus once the augmented sample set derived from high-density point clouds reaches roughly ***80–100*** plots.
- Similarly, when the number of field-measured individual trees reaches about ***70-100***, the model's accuracy likewise stabilizes.

6. Overview of Chinese YSs research

- **The effect of individual tree segmentation errors on the accuracy of biomass estimation**

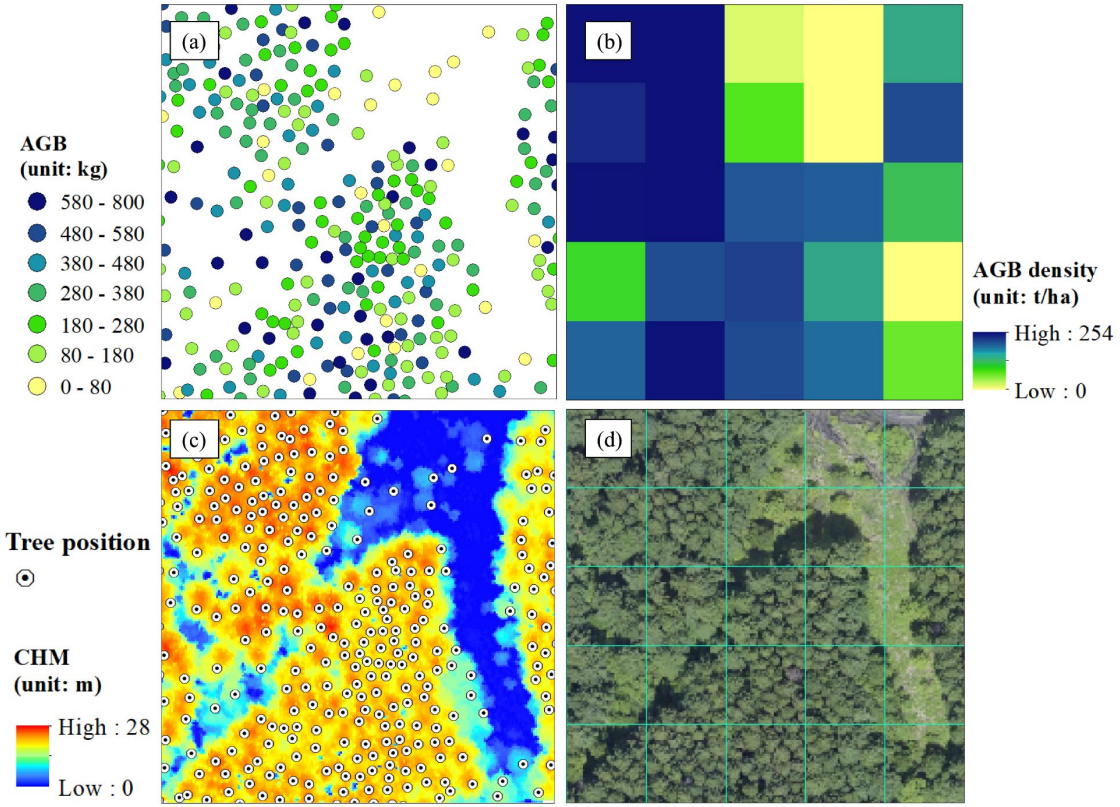


Simulating the effects of individual-tree segmentation errors on ITS–ABA biomass estimation models



Plot-scale AGB variation rates estimated by the LBI method under different individual-tree segmentation error scenarios.

6. Overview of Chinese YSs research

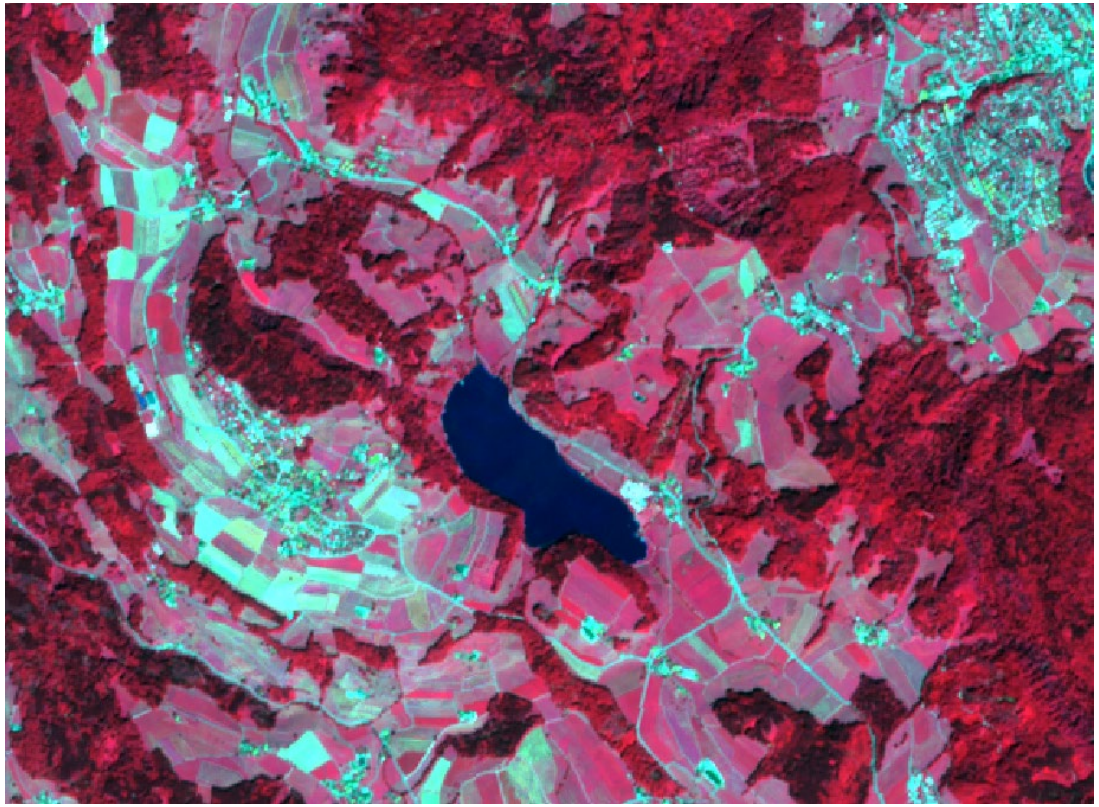


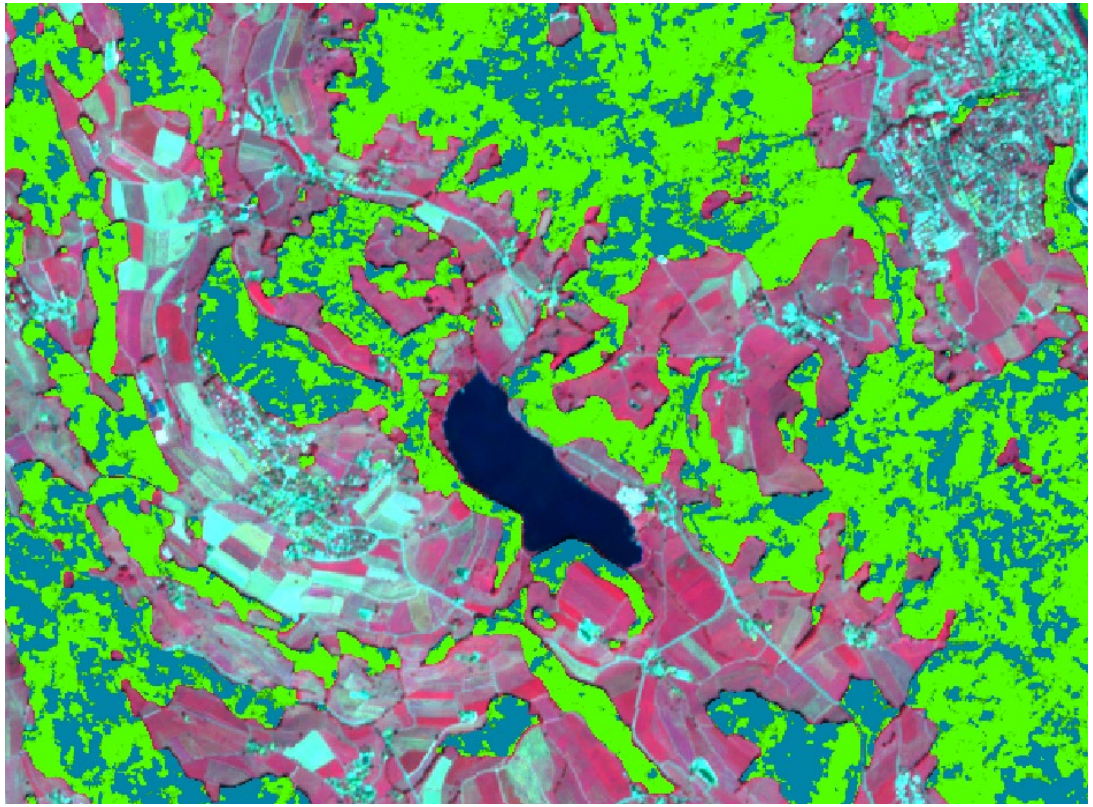
- Nationwide LBI-Based Canopy Biomass Model
- Accurate Individual-Tree Segmentation and Classification in Natural Forests
- Extending Applications to Satellite Platforms

Aerial LiDAR is All You Need!

6. Overview of European YSs research

1. classification of forest type based on multiple source datasets

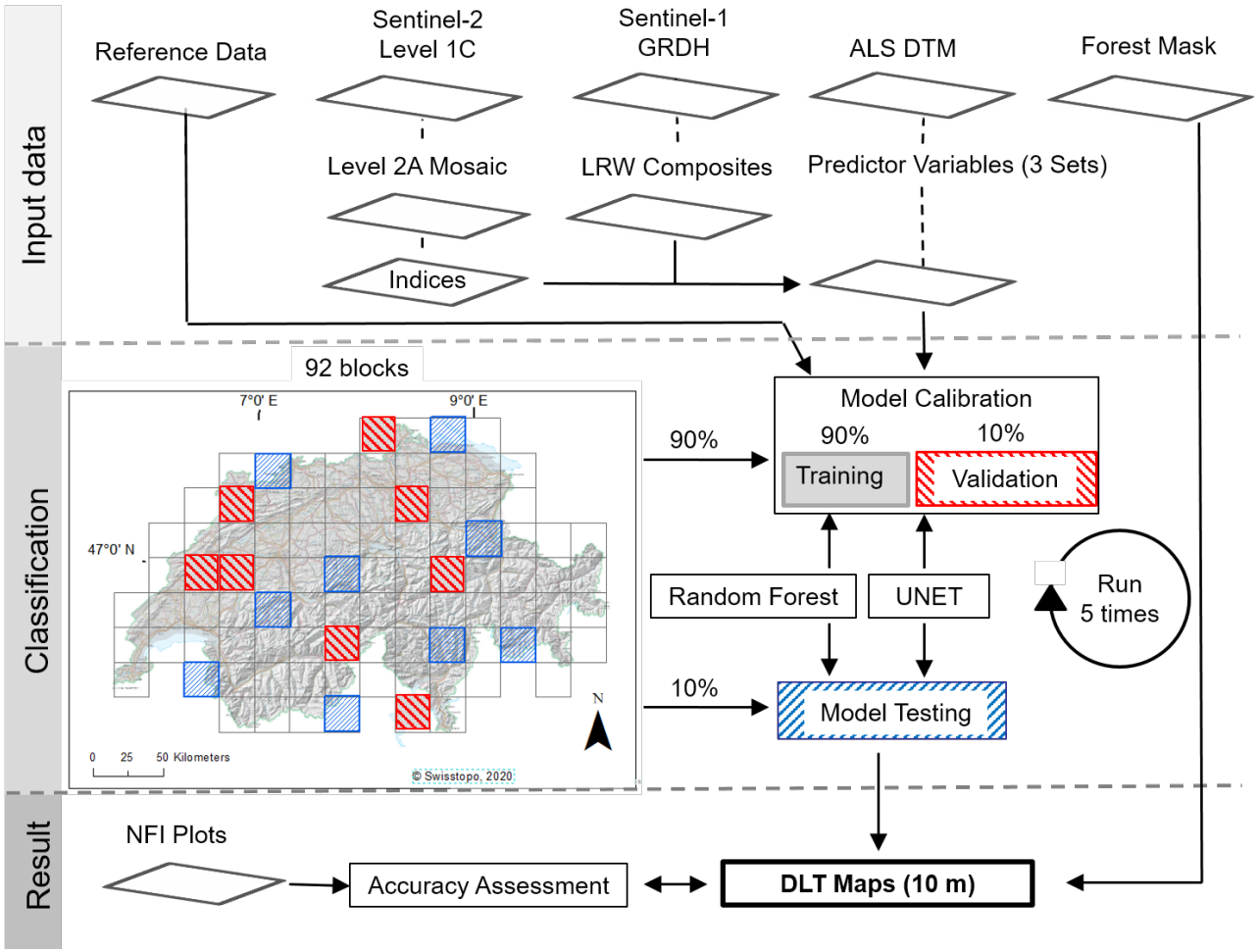




6. Overview of European YSs research

1. classification of forest type based on multiple source datasets

Workflow



Waser et al. (2021). ISPRS Journal of Photogrammetry and Remote Sensing, 180:209-226. *https://doi.org/10.1016/j.isprsjprs.2021.08.017*

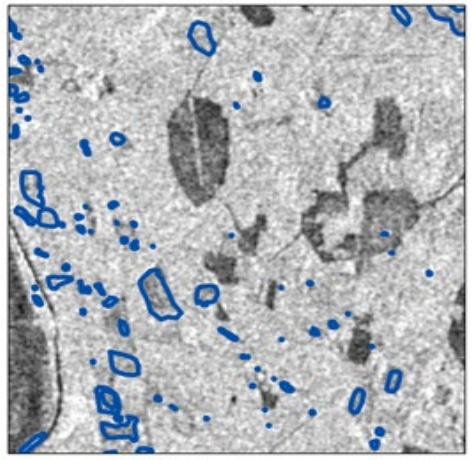
6. Overview of European YSs research

1. classification of forest type based on multiple source datasets

Input data

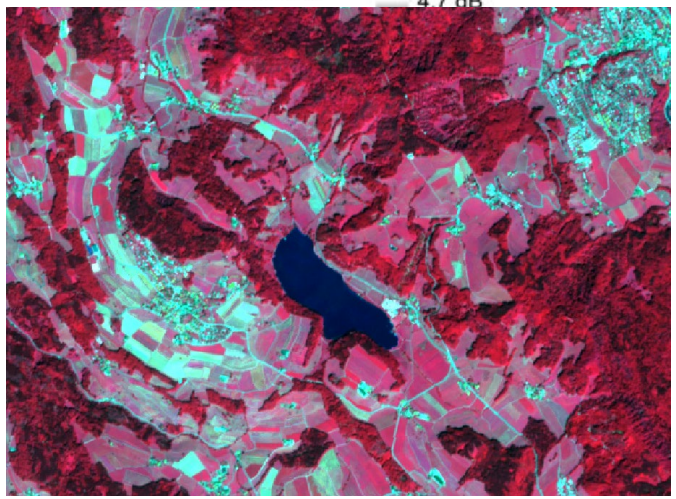
Sentinel-1

- C-Band Synthetic Aperture Radar (SAR)
- Spatial resolution: ~10 m
- VV and VH backscatter signals
- Temporal resolution: ~3-6 days
- Processing done by David Small (RSL)



Sentinel-2

- Level-2A (BOA)
- Spatial resolution: 10-20 m
- 10 (13) bands
- Temporal resolution: ~3-6 days



Digital Terrain Model (DTM)

- SwissAlti3D, 1 m (aspect, slope, elevation)

6. Overview of European YSs research

1. classification of forest type based on multiple source datasets

- **Variables from S1, S2 and DTM**

Source	Variables	Initial spatial resolution	Number of variables	Acquisition date	Set of predictors
S1	VV, VH	20	10	2021–2023	S1
S2	B2–B4, B8, B5–B7 B8A, B11, B12	10 20	4 6	2021–2023	S2
S2	GEMI, MSAVI, NDVI	10, 20	3	2021–2023	S2
DTM	E, A, S	1	3	2015–2018	EAS

- **3 Sets of variables:** S1+EAS (1)
  S2+EAS (2)
  S1S2+EAS (3)

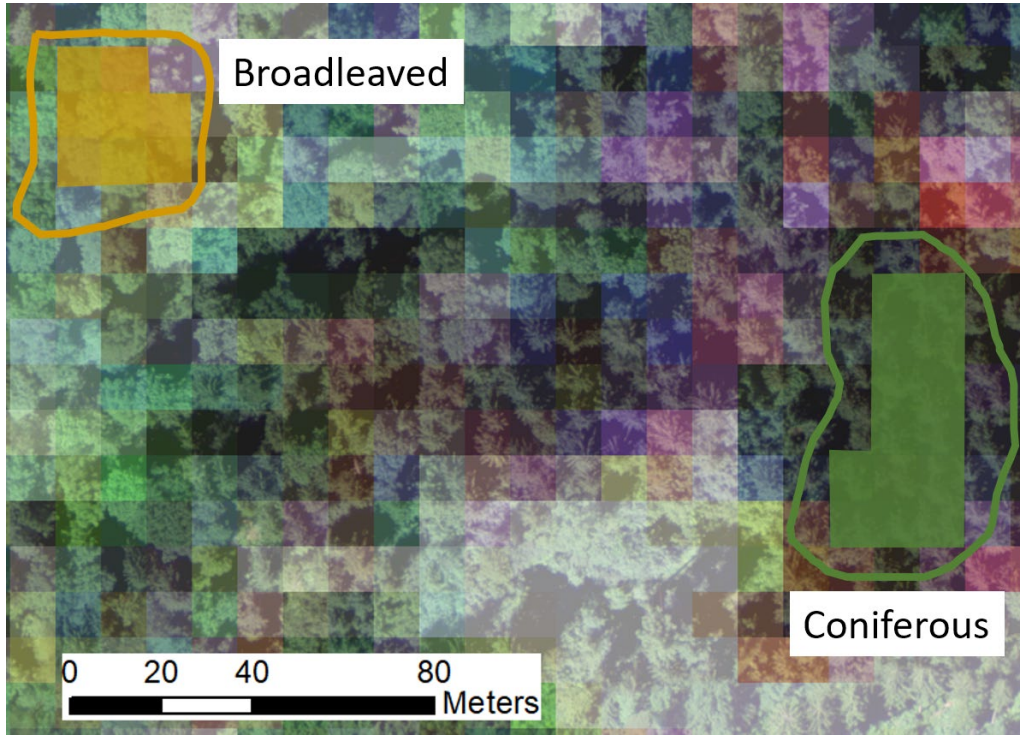
Forest Type NFI 2023 data set

6. Overview of European YSs research

1. classification of forest type based on multiple source datasets

Reference data

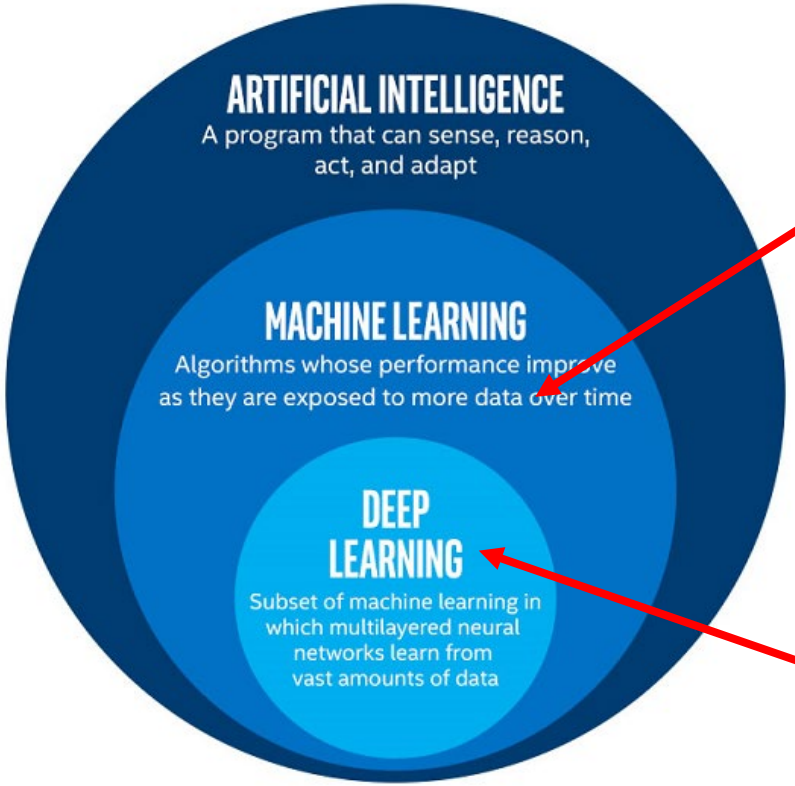
- Digitized polygons from aerial images
- broadleaved pixels (110 k), coniferous pixels (80 k)



6. Overview of European YSs research

1. classification of forest type based on multiple source datasets

Random forest & UNET



Random Forest (RF)
(Breiman 2012)

- ensemble learning classifier
- multiple decision trees

UNET
(Ronneberger et al. 2015)

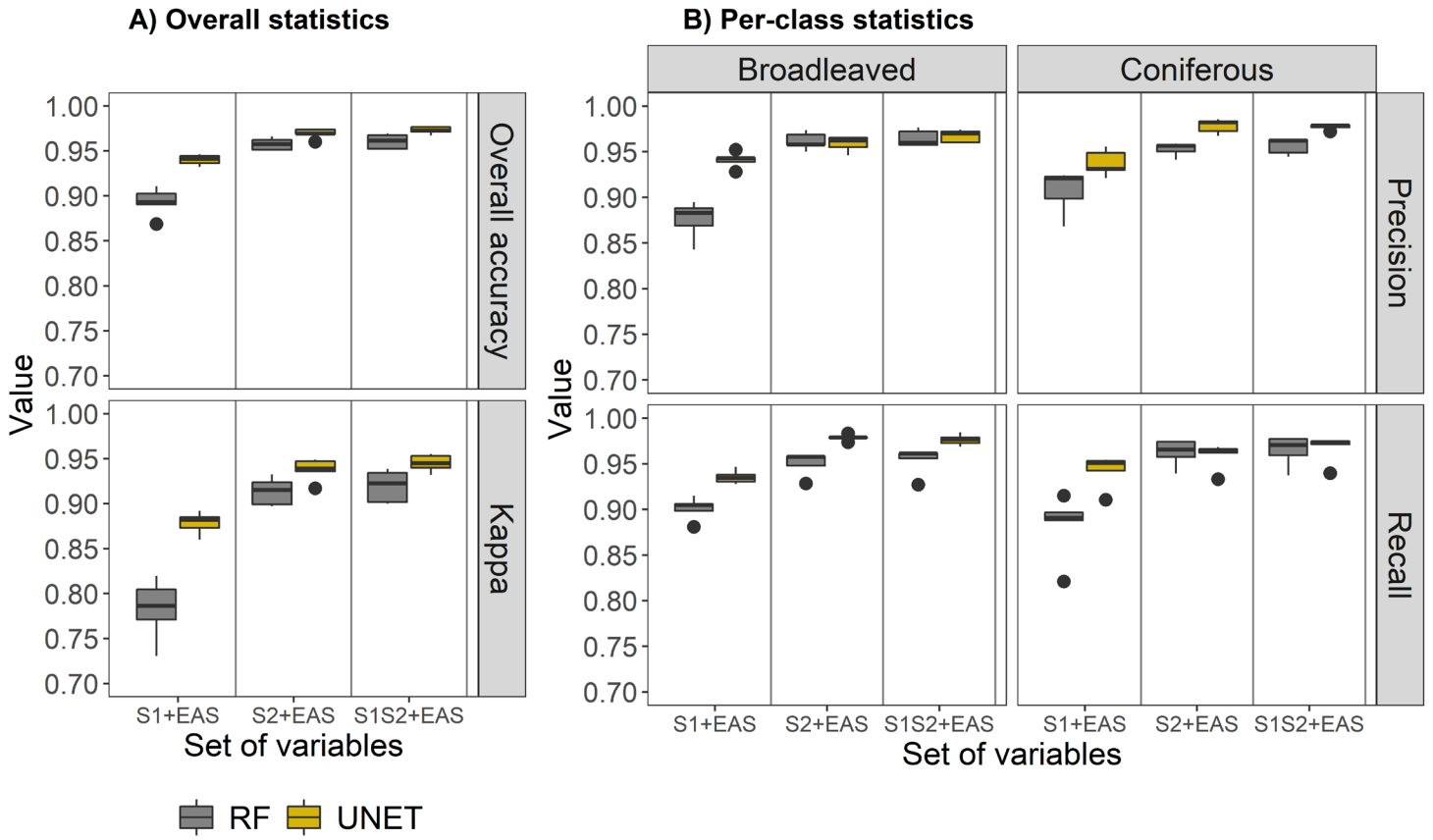
- fully convolutional network

While RF requires the hand-engineered predictor extraction (e.g. vegetation indices, textural variables) (Belgiu and Drăguţ, 2016) UNET "learns" directly from the input data to the target prediction (LeCun et al., 2015; Schmidhuber, 2015)

6. Overview of European YSs research

1. classification of forest type based on multiple source datasets

Model accuracies



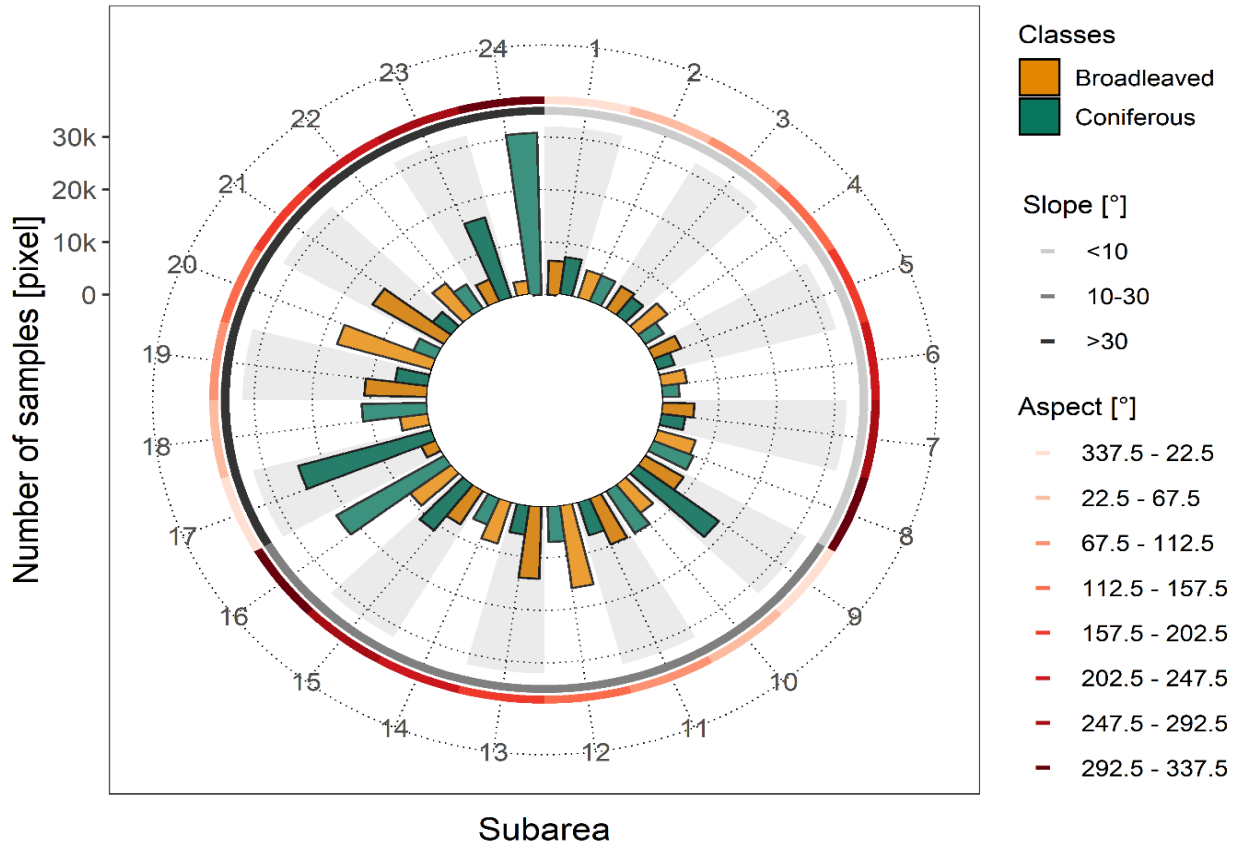
- RF and UNET overall performed very similarly (Kappa 0.95) when using all predictors from S1, S2 and DTM data
- UNET outperformed RF when using predictors from S1 and DTM data alone
- Small differences in model performance between single use of S2+DTM and combined S1+S2 and DTM data

6. Overview of European YSs research

1. classification of forest type based on multiple source datasets

Subarea-wide accuracy assessment

- 24 subareas to show small differences between model performances



6. Overview of European YSs research

1. classification of forest type based on multiple source datasets

Prediction (Map) accuracies

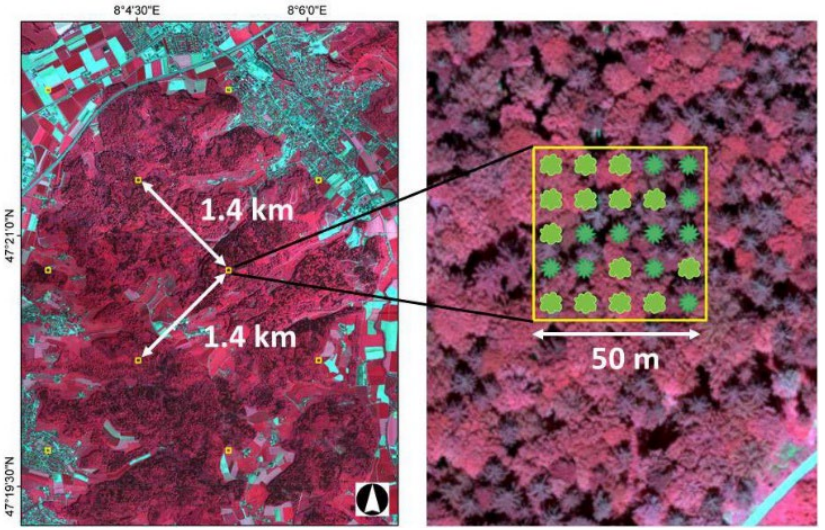
Comparison with independent NFI aerial image interpretation

- 3,173 plots
- RF and UNET overall similar: Kappa ~0.6, OA: 0.8, SD: 0.22
- Lower accuracies in ‘’mixed’’ plots

Comparison with Copernicus HRL DLT 2018

- Lower (~5%) accuracies for Copernicus data obtained
- (exception: class ‘’broadleaved > 80%’’)

Visual inspection

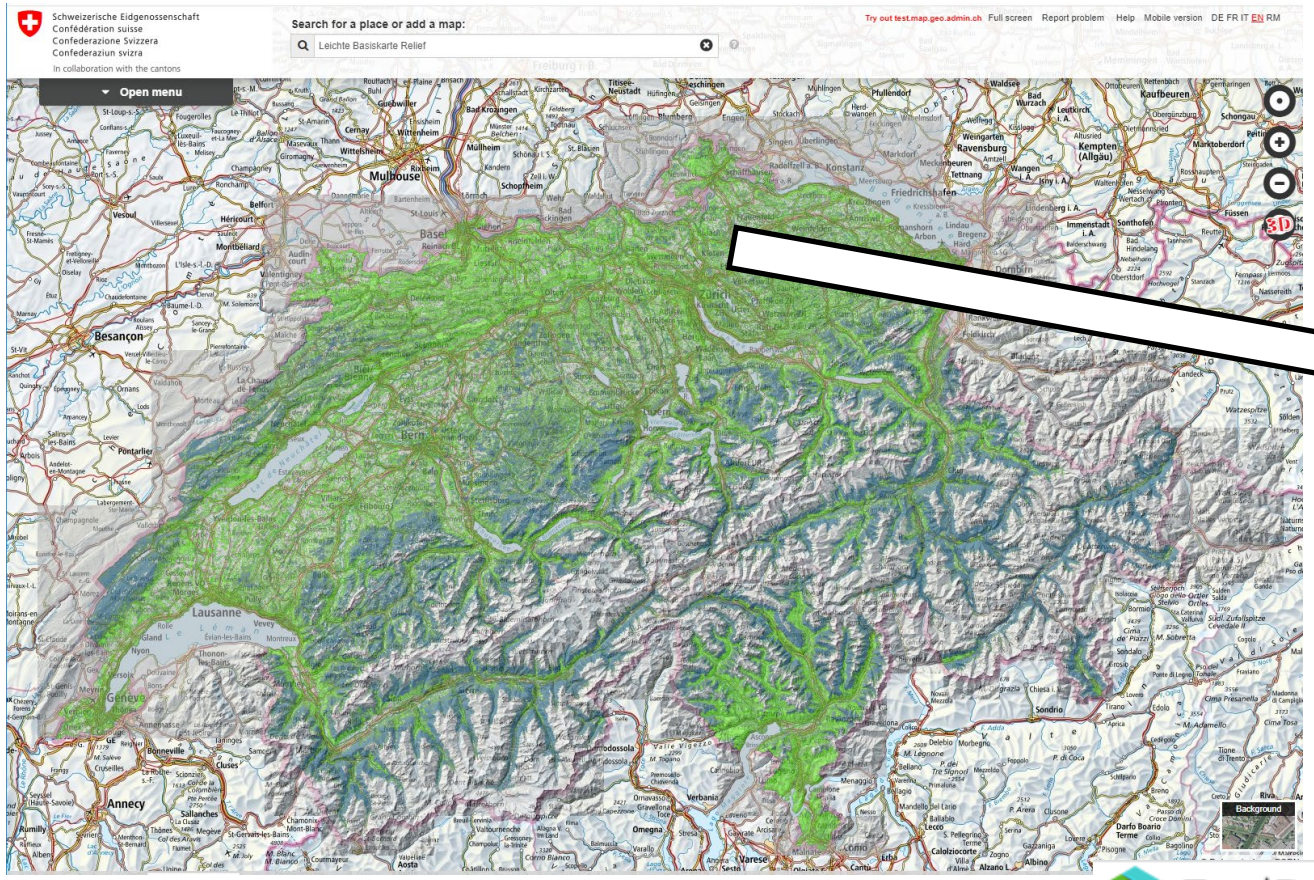


6. Overview of European YSs research

1. classification of forest type based on multiple source datasets

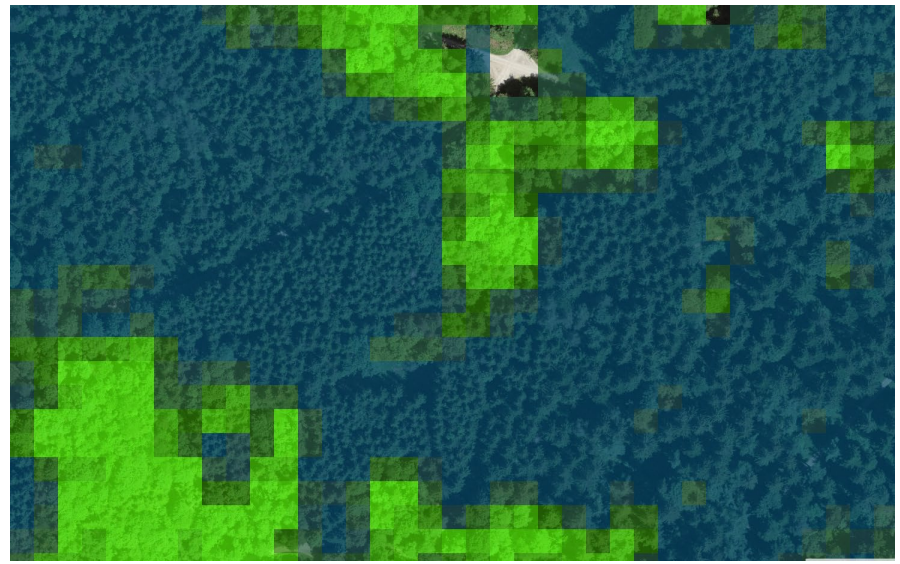
Dominant Leaf Type (DLT)

OA, Kappa; Precision / Recall > 0.95



Availabel: https://map.geo.admin.ch or <envidat.ch

Method: RF, Sentinel-1/-2 images, LiDAR, 400k Training data, 10m spatial resolution



0 ——— 100m

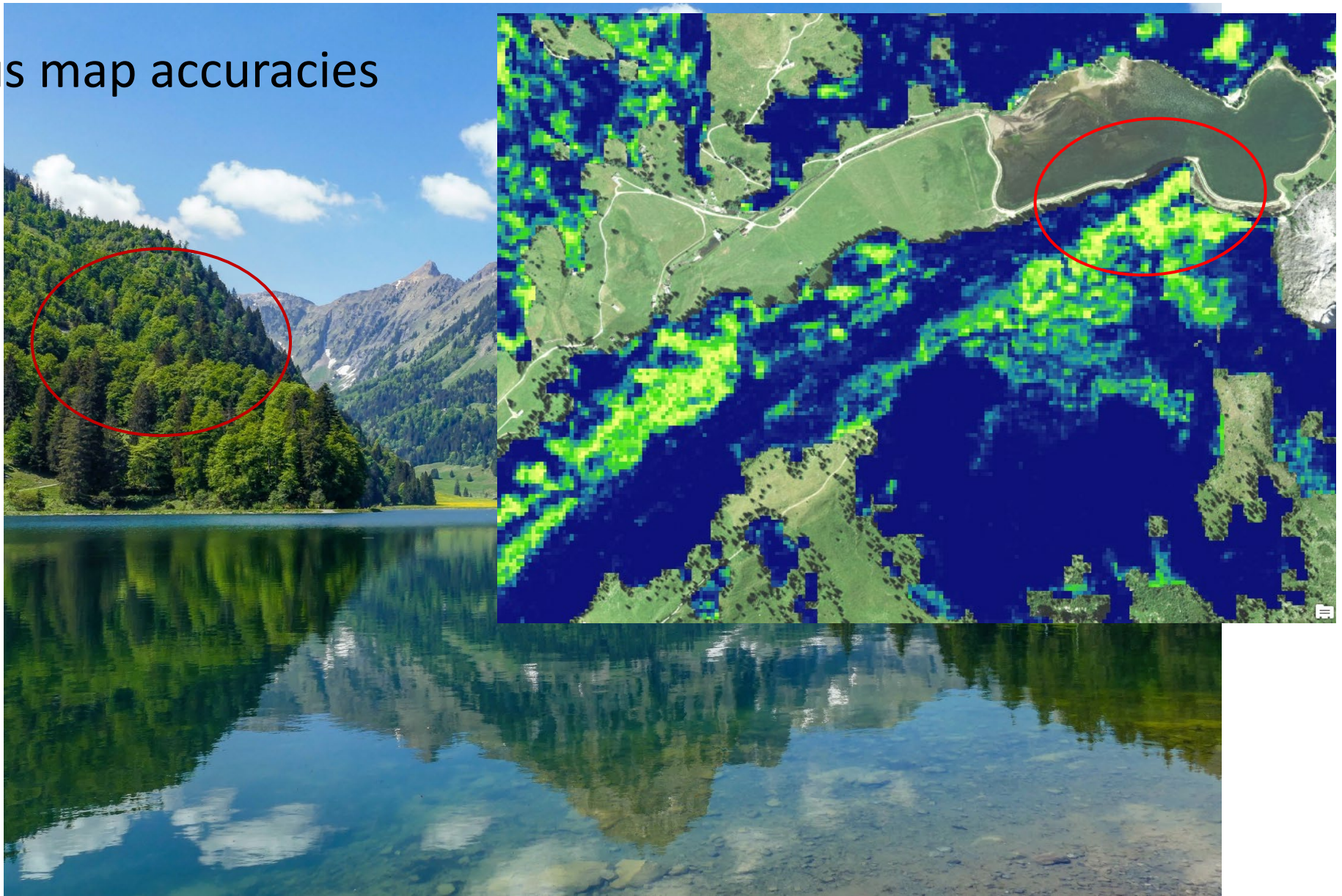
0 100%

Probability of deciduous tress

Waser et al. (2021). ISPRS Journal of Photogrammetry and Remote Sensing, 180:209-226. https://doi.org/10.1016/j.isprsjprs.2021.08.017

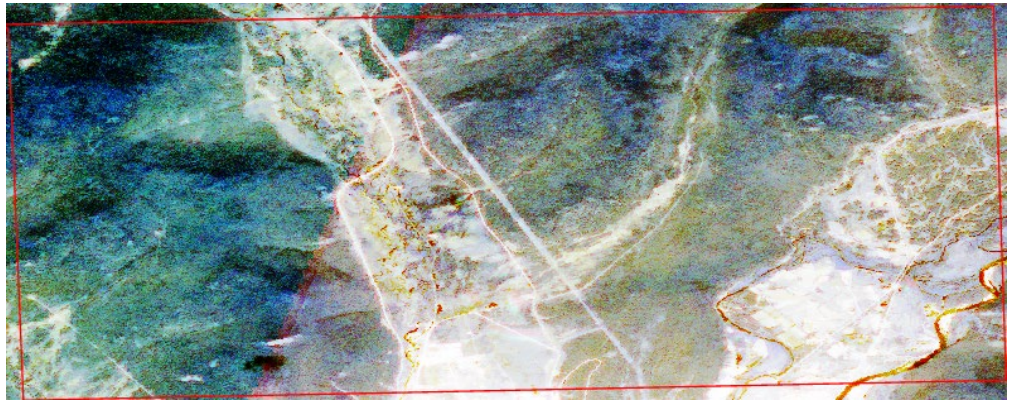
6. Overview of European YSs research

Model versus map accuracies

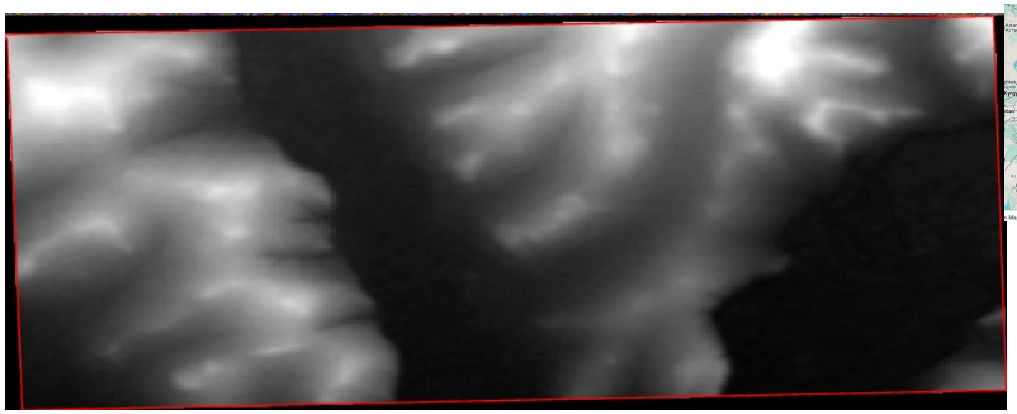


6. Overview of European YSs research

1. classification of forest type based on multiple source datasets

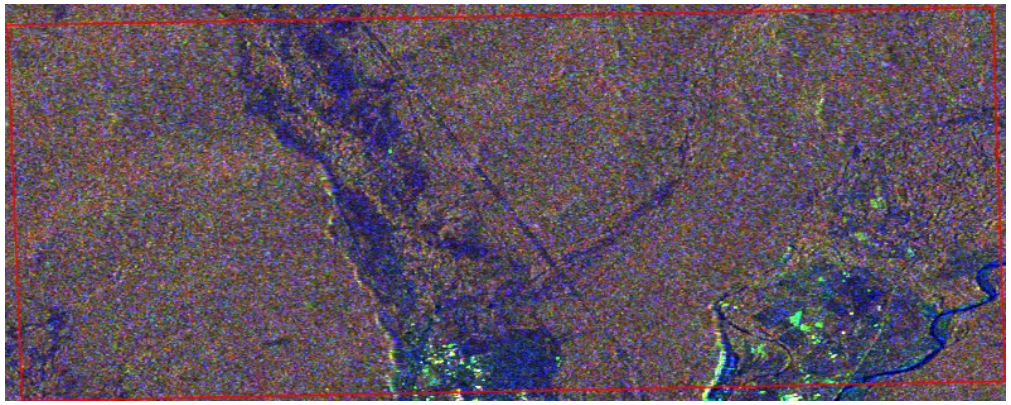


Sentinel -2 (2021 mosaic)

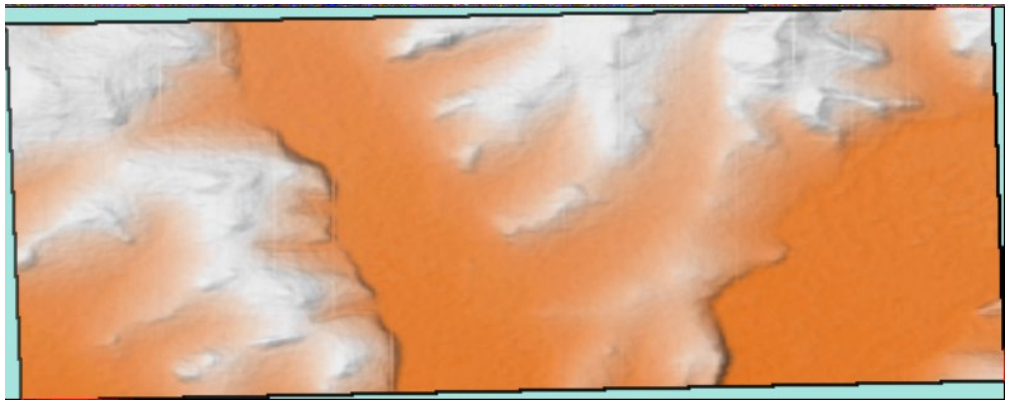




DEM (STRM)



Sentinel -1(2019 -2021)



Shaded Relief

6. Overview of European YSs research

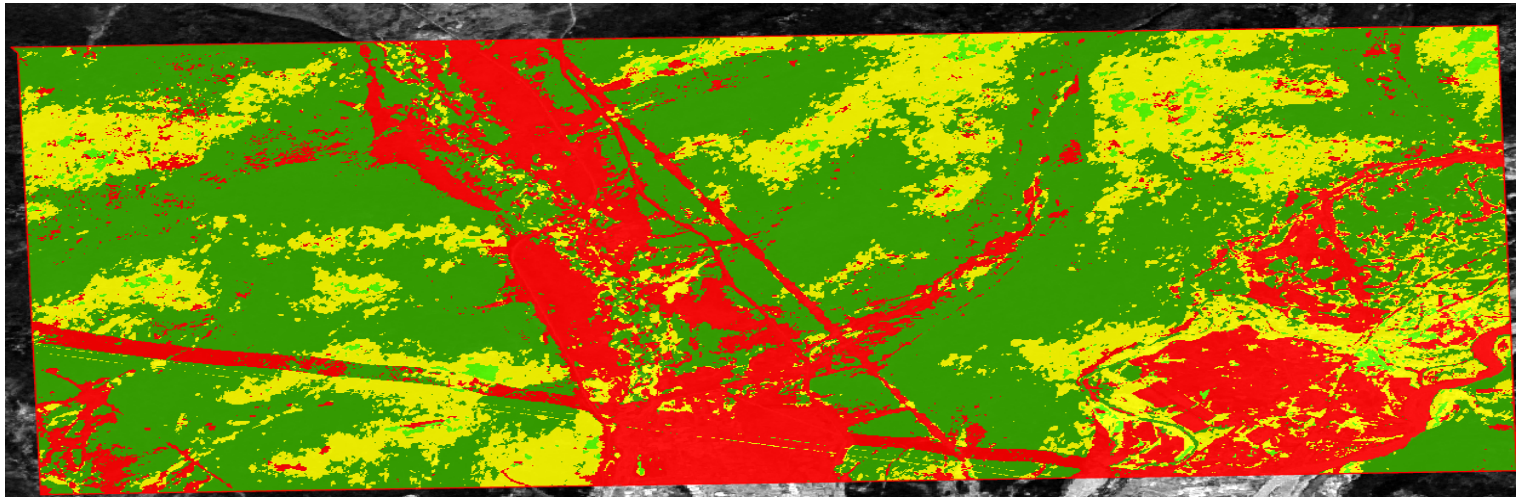
DLT mapping result



Dominant Leaf Type
(DLT)

9000 broadleaf

0 conifer

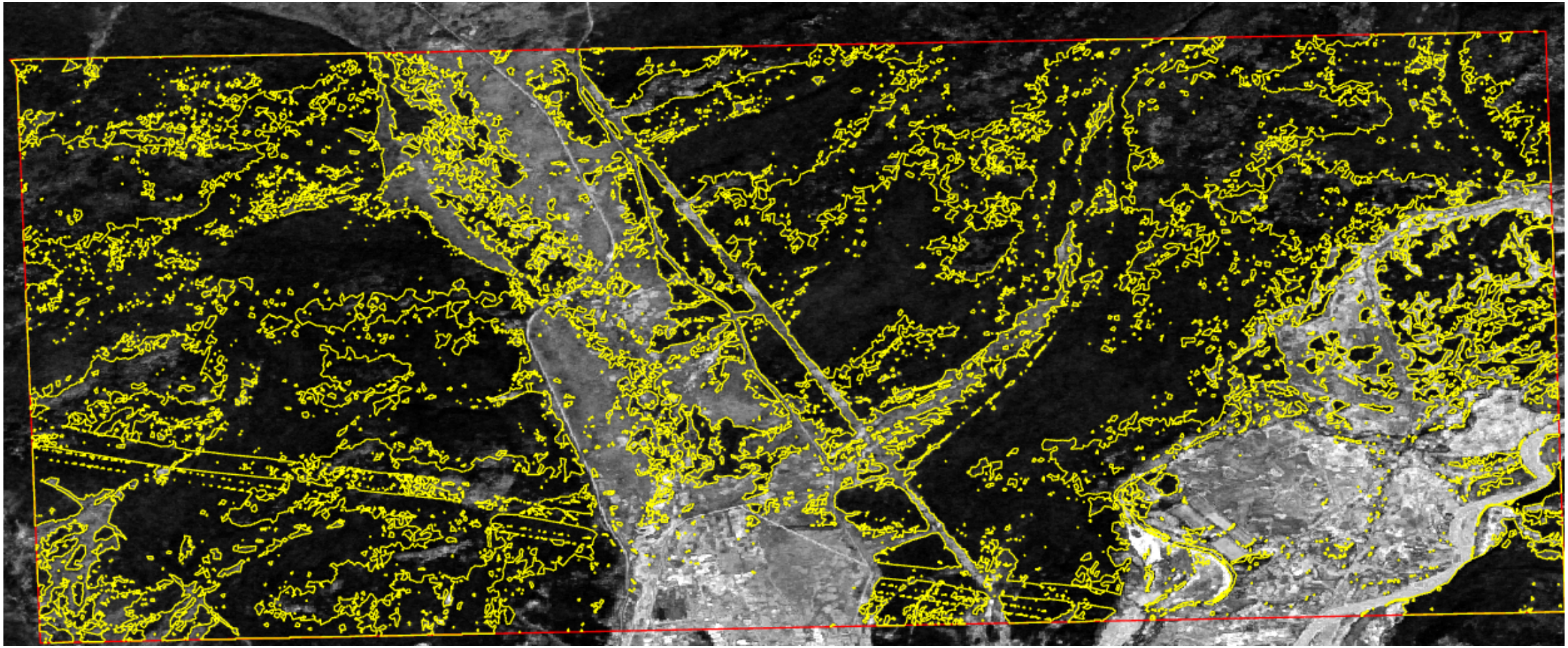


Forest Type by RF model

- conifer
- broadleaf
- mixture
- others

6. Overview of European YSs research

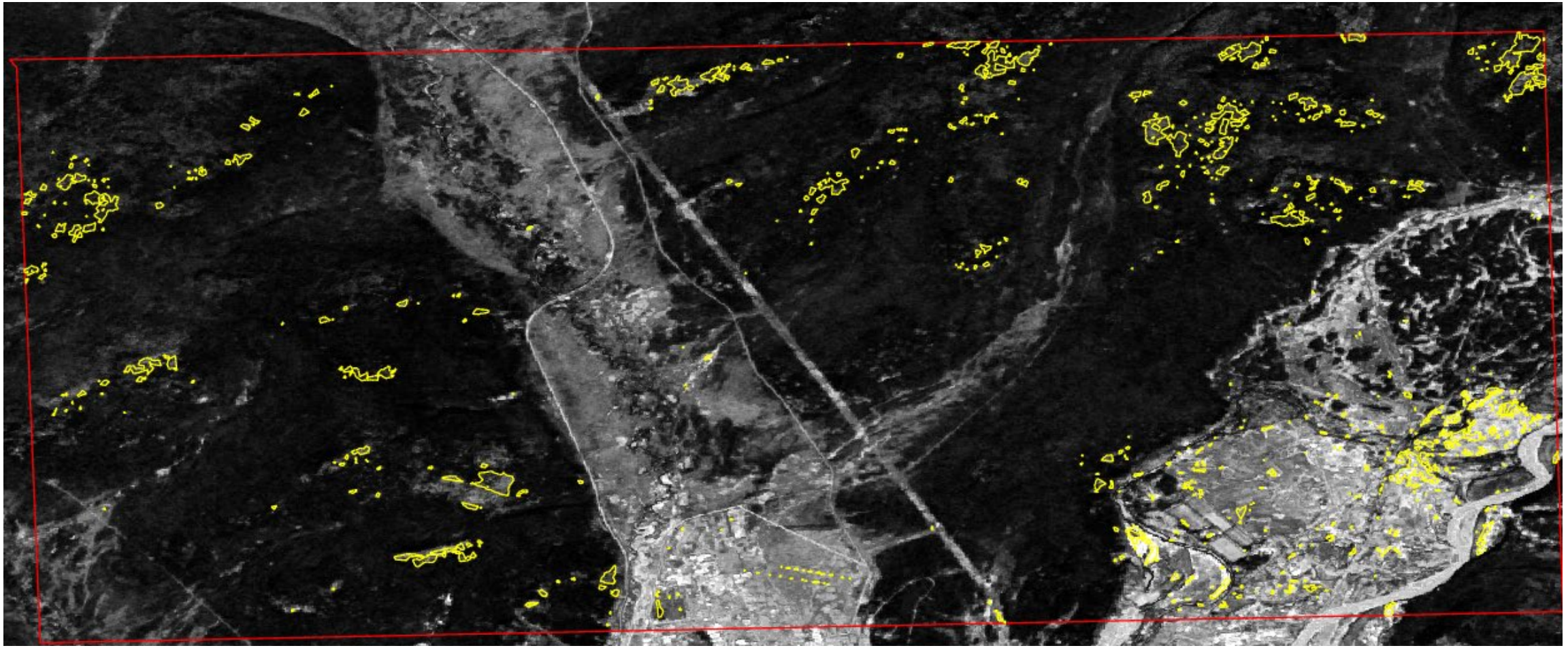
Conifer forest



bg: DLT — Inside conifer by RF

6. Overview of European YSs research

Broadleaf forest



bg: DLT — Inside broad leaf by RF

6. Overview of European YSs research

Conclusion

- Reliable predictions from countrywide (Swiss) to forest stand level were achieved by using S1S2+EAS - regardless of the use of RF or UNET
- The value predicted by Swiss DLT model in Genhe is lower for conifer forest and higher for broadleaf forest where the forest type is classified by RF model
- The threshold for conifer and broadleaf forest differs depending on the study region (Switzerland vs. China)
- Additional ground truth data is required to improve the Swiss DLT model across the whole range of forest ecosystems
- Forest types can be extracted based on the distribution/pattern of DLT pixel value



CSTEC
中国科学技术交流中心
China Science and Technology Exchange Center

esa
THE EUROPEAN SPACE AGENCY

IFRIT

WSL

Thank you